Journal of Cellular Biochemistry 94:917–943 (2005)

ARTICLES

Molecular and Functional Comparison of 1,25-Dihydroxyvitamin D_3 and the Novel Vitamin D Receptor Ligand, Lithocholic Acid, in Activating Transcription of Cytochrome P450 3A4

Peter W. Jurutka, Paul D. Thompson, G. Kerr Whitfield, Kristina R. Eichhorst, Neal Hall, Carlos Encinas Dominguez, Jui-Cheng Hsieh, Carol A. Haussler, and Mark R. Haussler*

Department of Biochemistry and Molecular Biophysics, University of Arizona College of Medicine, Tucson, Arizona 85724

Abstract The vitamin D receptor (VDR) binds to and mediates the effects of the 1,25-dihydroxyvitamin D_3 ($1,25(OH)_2D_3$) hormone to alter gene transcription. A newly recognized VDR ligand is the carcinogenic bile acid, lithocholic acid (LCA). We demonstrate that, in HT-29 colon cancer cells, both LCA and $1,25(OH)_2D_3$ induce expression of cytochrome P450 3A4 (CYP3A4), an enzyme involved in cellular detoxification. We also show that LCA-VDR stimulates transcription of gene reporter constructs containing DR3 and ER6 vitamin D responsive elements (VDREs) from the human *CYP3A4* gene. Utilizing gel mobility shift, pulldown, and mammalian two-hybrid assays, we observe that: (i) $1,25(OH)_2D_3$ enhances retinoid X receptor (RXR) heterodimerization with VDR more effectively than LCA, (ii) the $1,25(OH)_2D_3$-liganded VDR-RXR heterodimer recruits full-length SRC-1 coactivator, whereas this interaction is minimal with LCA unless LXXLL-containing fragments of SRC-1 are employed, and (iii) both $1,25(OH)_2D_3$ and LCA enhance the binding of VDR to DRIP205/mediator, but unlike $1,25(OH)_2D_3$-VDR, LCA-VDR does not interact detectably with NCoA-62 or TRIP1/SUG1, suggesting a different pattern of LCA-VDR comodulator association. Finally, residues in the human VDR (hVDR) ligand binding domain (LBD) were altered to create mutants unresponsive to $1,25(OH)_2D_3$- and/or LCA-stimulated transactivation, identifying S237 and S225/S278 as critical for $1,25(OH)_2D_3$ and LCA action, respectively. Therefore, these two VDR ligands contact distinct residues in the binding pocket, perhaps generating unique receptor conformations that determine the degree of RXR and comodulator binding. We propose that VDR is a bifunctional regulator, with the $1,25(OH)_2D_3$-liganded conformation facilitating high affinity endocrine actions, and the LCA-liganded configuration mediating local, lower affinity cellular detoxification by upregulation of CYP3A4 in the colon. J. Cell. Biochem. 94: 917–943, 2005.

Key words: colon cancer; detoxification; vitamin D responsive elements; retinoid X receptor; coactivators; mediator; ligand-generated nuclear receptor conformation

The traditional role of vitamin D, via its 1,25-dihydroxyvitamin D_3 ($1,25(OH)_2D_3$) hormonal metabolite, is to effect calcium and phosphate homeostasis, ensuring that the concentration of these ions is sufficient to promote bone mineralization and remodeling [Haussler et al., 1998; Jones et al., 1998]. Acting primarily in the small intestine, $1,25(OH)_2D_3$ binds to the nuclear vitamin D receptor (VDR), with liganded VDR eliciting the transcription of genes encoding proteins that facilitate calcium and phosphate absorption [Haussler et al., 1998; Christakos et al., 2003]. $1,25(OH)_2D_3$ also exerts direct effects on bone via association with VDR in

Peter W. Jurutka and Paul D. Thompson have contributed equally to this work.

Grant sponsor: National Institutes of Health; Grant numbers: DK33351, DK063930.

Peter W. Jurutka's present address is Department of Integrated Natural Sciences, Arizona State University West, Phoenix, AZ 85069.

Paul D. Thompson's present address is Department of Life and Health Sciences, School of Biomedical Sciences, University of Ulster, Coleraine, Northern Ireland.

*Correspondence to: Mark R. Haussler, Department of Biochemistry and Molecular Biophysics, College of Medicine, University of Arizona, Tucson, AZ 85724.
E-mail: haussler@u.arizona.edu

Received 28 September 2004; Accepted 8 October 2004

DOI 10.1002/jcb.20359

osteoblasts to stimulate transcription of the gene coding for the receptor activator of NF-κB ligand (RANKL) [Kitazawa and Kitazawa, 2002], which acts on osteoclast precursor cells in a paracrine fashion to trigger their differentiation into bone-resorbing osteoclasts [Boyle et al., 2003]. Other osteoblast-expressed genes transcriptionally activated by $1,25(OH)_2D_3$-VDR include those encoding osteocalcin [Markose et al., 1990; Terpening et al., 1991] and osteopontin [Noda et al., 1990], two proteins involved in bone remodeling.

The target tissues for the $1,25(OH)_2D_3$ hormone and nuclear VDR are not limited to bone and intestine, but are now known to encompass the central nervous and immune systems, several endocrine glands, muscle, and terminally differentiating epithelial cells such as those of the skin, indicating that the role of $1,25(OH)_2D_3$-VDR extends far beyond its classic calcemic and phosphatemic effects [Haussler et al., 1998; Jurutka et al., 2001; Sutton and MacDonald, 2003]. In many of these tissues, $1,25(OH)_2D_3$ induces 25-hydroxyvitamin D_3 24-hydroxylase (CYP24), the enzyme responsible for 24-hydroxylation of vitamin D metabolites [Ohyama et al., 1996], to initiate the major pathway for vitamin D catabolism [Haussler et al., 1998]. Thus, VDR knockout mice [Yoshizawa et al., 1997], as well as patients afflicted with hereditary hypocalcemic vitamin D-resistant rickets (HVDRR) caused by inactivating mutations in VDR [Malloy et al., 1999], display the phenotype of severe rickets and an inability to catabolize the $1,25(OH)_2D_3$ hormone. VDR null mice [Li et al., 1997] and, in some cases, HVDRR patients [Malloy et al., 1999] also exhibit dermal cysts and alopecia, indicating that VDR is required for proper skin differentiation and hair cycling, respectively. Finally, mounting evidence implicates $1,25(OH)_2D_3$ as an epithelial cell anti-cancer and chemopreventative agent [Guyton et al., 2001]. Several cancers, including those of the breast, prostate, and colon are thought to be influenced by vitamin D status [Guyton et al., 2001]. The $1,25(OH)_2D_3$ ligand and select synthetic analogs of vitamin D are known to possess potent anti-proliferative, prodifferentiation, proapoptotic, and/or cell cycle arrest activities in epithelial cells. The molecular mechanisms underlying these effects are not known but may be related to the ability of liganded VDR to arrest cells at the G1 stage via induction of cell cycle regulatory proteins p21 and p27, to control cell growth transcription factors such as c-*myc* and c-*fos*, or to elicit apoptosis by repression of the *Bcl*-2 anti-apoptotic factor [Haussler et al., 1998].

Another mechanism for the chemoprotective effect of $1,25(OH)_2D_3$-VDR is induction of cytochrome P450 heme-containing monooxygenases (CYPs), enzymes involved in cellular clearance of deleterious hydrophobic xeno- and endobiotic compounds [Honkakoski and Negishi, 2000; Chawla et al., 2001]. This includes VDR-mediated induction of the aforementioned CYP24 to initiate $1,25(OH)_2D_3$ catabolism [Ohyama et al., 1996], as well as regulation of CYP3A4 and CYP2B [Schmiedlin-Ren et al., 2001; Drocourt et al., 2002; Thompson et al., 2002; Pascussi et al., 2003]. Thus, VDR-mediated induction of CYP detoxification enzymes could increase the metabolic elimination of potentially carcinogenic compounds.

A newly recognized role of VDR is that of a low affinity sensor for bile acids, specifically the secondary bile acid, lithocholic acid (LCA) [Makishima et al., 2002]. LCA is a carcinogenic compound formed via bacterial 7-dehydroxylation of the primary bile acid, chenodeoxycholic acid (CDCA). LCA has been implicated in the progression of colon cancer [Kawaura et al., 1989; Hamada et al., 1994], an action that can be partially inhibited by administration of the 1α(OH)-vitamin D_3 synthetic precursor of $1,25(OH)_2D_3$ [Kawaura et al., 1989]. High fat diets increase the synthesis and secretion of primary and secondary bile acids, with LCA being the most toxic and also the least absorbed into the enterohepatic circulation, passing readily into the colon [Nagengast et al., 1995]. The significance of LCA activation of VDR in the context of CYP induction is that both $1,25(OH)_2D_3$ and LCA, acting as VDR ligands, could induce the expression of *CYP* genes in the colonocyte to effect LCA detoxification.

In the first phase of the present study, we evaluated the ability of either $1,25(OH)_2D_3$ or LCA ligands to induce human *CYP3A4* in small intestine and colon cancer cells, and tested a series of candidate responsive elements in the promoter region of this gene for their ability to bind liganded VDR and mediate transcriptional activation in several cellular contexts. In the second phase of the current experiments, we probed whether the molecular mechanism

whereby LCA-liganded VDR promotes gene transcription might be distinct from that of the classic $1,25(OH)_2D_3$ ligand. Mutagenesis of the VDR ligand binding domain (LBD) was employed to define unique amino acid residues involved in $1,25(OH)_2D_3$- and/or LCA-mediated transcriptional activation of *CYP3A4*. Also, we assessed the ability of $1,25(OH)_2D_3$- and LCA-liganded VDR to interact with the retinoid X receptor (RXR) heteropartner [Kliewer et al., 1992; MacDonald et al., 1993], as well as a selection of nuclear receptor coactivators [Xu and Li, 2003], attempting to gain insight into the downstream events following liganding of VDR by $1,25(OH)_2D_3$ or LCA.

Although the precise mechanism whereby liganded VDR stimulates target gene transcription has yet to be completely characterized, there is a current model derived from previous VDR studies [Jurutka et al., 2001], as well as concepts elucidated for other nuclear receptors [Rosenfeld and Glass, 2001]. In this context, VDR can be considered a typical nuclear hormone receptor [Jurutka et al., 2001], comprised of a dual zinc finger-based DNA binding domain (DBD), nuclear localization signal(s), and a LBD which binds the cognate ligands [Makishima et al., 2002]. Further, VDR is a member of the thyroid hormone, retinoic acid, oxycholesterol, and xenobiotic subfamily of nuclear receptors that primarily heterodimerizes with RXR in order to recognize direct repeat responsive elements in the promoters of regulated genes [Whitfield et al., 1999; Chawla et al., 2001; Lu et al., 2001]. Most known vitamin D responsive elements (VDREs) consist of a hexanucleotide direct repeat separated by three base pairs (DR3) [Haussler et al., 1998]. The predominant surface for human VDR (hVDR) association with RXR is found on the LBD [Bourguet et al., 1995; Haussler et al., 1998; Rochel et al., 2000], and naturally occurring mutations in this region confer the HVDRR clinical phenotype [Whitfield et al., 1996], providing strong evidence for an obligatory structural interplay between VDR ligand binding and RXR heterodimerization that leads to selective VDRE association.

In addition to binding lipophilic ligands and heterodimerizing with RXRs [Nakajima et al., 1994; Whitfield et al., 1995], the LBD of VDR contains an activation function-2 (AF-2) located near the C-terminus of the receptor [Haussler et al., 1998]. Upon liganding, the AF-2 of nuclear receptors pivots into a closed position to create a hydrophobic cleft for attraction of comodulators with LXXLL motifs [Vanhooke et al., 2004]. LXXLL-possessing VDR coactivators of the p160 class encompass steroid receptor coactivator-1 (SRC-1) [Oñate et al., 1995; Gill et al., 1998], glucocorticoid receptor (GR) interacting protein 1 (GRIP1 or SRC-2) [Hong et al., 1997], and the activator of thyroid hormone and retinoic acid receptors (ACTR or SRC-3) [Chen et al., 1997]. Members of this SRC/p160 class of coactivators, as well as the associated cointegrator, CBP, possess histone acetyl transferase (HAT) activity [McKenna et al., 1999b] for remodeling of chromatin structure within the promoter region of hormone responsive genes. Recent studies of the rat osteocalcin promoter reveal that VDR binding to the VDRE is required for enhanced acetylation of histones H3 and H4 downstream of the VDRE [Gutierrez et al., 2004]. Also, a large mediator complex containing VDR interacting proteins (DRIPs) [Rachez et al., 1999] participates in transcriptional control by VDR via association with the AF-2 of the receptor and bridging to RNA polymerase II, thereby stabilizing the transcriptional pre-initiation complex and directing its activity to the VDR controlled gene [Rachez et al., 1999; McKenna et al., 1999a]. Other VDR-interacting proteins that likely transduce the signal for transcriptional control include the Williams syndrome transcription factor that recruits a SWI/SNF-like intra-nucleosome chromatin modeling complex [Kitagawa et al., 2003], NCoA-62, which both attracts HATs and mediates hnRNA processing [Zhang et al., 2003], and the TRIP1/SUG1 director of VDR ubiquitination and eventual proteolysis [Masuyama and MacDonald, 1998].

In order to determine if $1,25(OH)_2D_3$ and LCA confer potentially different VDR conformations with measurable consequences for receptor function, we examined the ability of VDR bound to these ligands to interact with the RXR coreceptor, p160 coactivator HATs, DRIP205, NCoA-62, and TRIP1/SUG1. The results support a hypothesis that ligand induction of such target genes as *CYP3A4* by $1,25(OH)_2D_3$ and LCA provides two distinct, complementary molecular mechanisms for the role of VDR in mediating protection against the development of high fat Western diet-induced colon cancer, including that promoted by LCA.

MATERIALS AND METHODS

Plasmid Constructions

cDNAs encoding hVDR [Baker et al., 1988], human RXRα (hRXRα) [Mangelsdorf et al., 1990], and mouse glucocorticoid receptor (mGR) [Danielsen et al., 1989] were subcloned into the expression plasmid pSG5 [Green et al., 1988] as described [Hsieh et al., 1991]. Synthesis of VDR point mutants in full-length wild-type (WT) hVDR was accomplished using a QuikChange site-directed mutagenesis kit (Stratagene, La Jolla, California) according to the protocol of the manufacturer. All receptor mutants were confirmed by DNA sequencing. The human SRC-1 expression plasmid (pCR3.1-hSRC-1A) was kindly provided by Dr. Ming Tsai [Spencer et al., 1997], Baylor College of Medicine. The human NCoA-62 expression plasmid (pSG5-hNCoA-62) was a gift from Dr. Paul MacDonald [Baudino et al., 1998], Case Western Reserve University. A human DRIP205 expression construct (pcDNA3-hDRIP205) was kindly provided by Dr. Leonard Freedman [Rachez et al., 1998] from the Memorial Sloan-Kettering Cancer Center, and the human thyroid receptor interacting protein 1 [Lee et al., 1995] expression vector pCDM8-Flag-hTRIP1, was a gift from Dr. David Moore, Baylor College of Medicine. The SRC-1 and TRIP1 cDNAs were recloned into the pSG5 expression plasmid. EB1089 was a gift from Dr. Lise Binderup, Leo Pharmaceuticals (Ballerup, Denmark).

Transfection of Cultured Cells and Transcriptional Activation Assays

Each of the tested cell lines (see individual figure legends) were transfected with the indicated amount of WT pSG5-hVDR expression plasmid [Hsieh et al., 1991], mutant VDRs or, in some cases, expression plasmids for full-length RXRα, SRC-1, DRIP205, NCoA-62, or TRIP1 (described above) by the calcium phosphate-DNA coprecipitation method as detailed previously [Jurutka et al., 1993]. In addition, each plate (750,000 cells/60-mm plate) received various reporter plasmids containing two copies of a VDRE (see Fig. 2 for details and sequence of each VDRE) inserted upstream of the viral thymidine kinase promoter-growth hormone (GH) reporter gene (Nichols Institute, San Juan Capistrano, CA). A positive control reporter vector contained four copies of the rat osteocalcin (ROC) VDRE linked to growth hormone (ROC VDRE)[4]. The pTZ18U plasmid was used as carrier DNA and each transfection contained a constant amount of total DNA (20 μg). Sixteen-hours post-transfection, the cells were washed, then re-fed in Dulbecco's modified Eagle's medium (DMEM; Life Technologies, Inc., Grand Island, NY) supplemented with 10% fetal bovine serum (FBS), 100 units/ml penicillin, 100 μg/ml streptomycin, and 10^{-8} M $1,25(OH)_2D_3$, 10^{-4}–10^{-6} M of the indicated bile acid, or 10^{-5} M dexamethasone in ethanol vehicle. After 24 h of incubation at 37°C, the level of growth hormone secreted into the culture medium was assessed by radioimmunoassay using a commercial kit (Nichols Institute) according to the manufacturer's protocol. A parallel set of transfected cells containing only VDR expression plasmid and/or pTZ18U were utilized for preparation of cellular lysates for subsequent use in mRNA purification/reverse transcriptase-polymerase chain reaction (RT-PCR; HT-29 and Intestine-407 cells), Western blotting or gel mobility shift assays as described below.

Some transcription assays employed a luciferase-containing reporter vector (24-OHase-Luc) that was constructed by subcloning 5.5 kb of the promoter region [Jin et al., 1996] of the human *CYP24* gene (kindly provided by Dr. S. Christakos and Dr. J.W. Pike, New Jersey Medical School and University of Wisconsin, respectively) into a firefly luciferase plasmid, lucp1 [Jin et al., 1996]. The human *CYP24* gene possesses two antisense DR3 VDREs (with sequences $AGGTGAN_3AGGGCG$ and $AGTTCAN_3GGTGTG$ in the sense orientation) at −156 and −277 bp, respectively, relative to the transcription start site. These sequences in the human *CYP24* gene differ slightly in both position and sequence from the those in the rat gene (Fig. 2); the species source for each *CYP24* VDRE in the various experiments is listed in the pertinent figure legend. COS-7 cells (50,000 cells/well in 24-well plates) were transfected with 200 ng/well of p24-OHase-Luc, 10 ng/well of pRL-Null, 20 ng/well of pSG5-hVDR, or VDR mutants, either in the absence or presence of various ligands. The Renilla luciferase (RL) construct was included as a non-regulated gene. After 24 h, cells were washed twice with PBS and lysed with 150 μl passive lysis buffer. Firefly and RL activities were measured sequentially from each well using a Sirius Luminometer (Pforzheim, Germany) and

DLR assay reagents (Promega, Madison, WI) per the manufacturer's instructions. The ratio of firefly to RL activity was calculated to normalize for transfection efficiency.

Isolation of mRNA and RT-PCR Analysis

HT-29 and Intestine-407 cells were transfected as described above and cells (2×10^7) were harvested by trypsinization followed by cell lysis in detergent-based buffers and purification of mRNA using a commercial kit (Oligotex Direct mRNA; Qiagen, Valencia, Ca) according to the manufacturer's protocol. RT-PCR analysis was performed using primers described previously [Schmiedlin-Ren et al., 1997] and employing a commercial RT-PCR kit (ProStar; Stratagene, La Jolla, CA). First strand cDNA synthesis reactions included 1–2 ng of purified mRNA from each cell type and hormone treatment and an oligo(dT) primer. Reactions were heated to 65°C for 5 min followed by cooling to room temperature, addition of first strand buffer, RNase inhibitor, dNTPs, and 5 U of Stratascript reverse transcriptase. First strand synthesis proceeded at 42°C for 70 min followed by heat inactivation for 1 min at 95°C. PCR reactions contained 1 μl of the first strand (cDNA) reaction mixture, 5 μl *Taq* DNA polymerase buffer, 0.4 μl dNTPs, 1.0 μl each of primers [Schmiedlin-Ren et al., 1997] designed specifically for human CYP3A4 (5′-CCT TAC ATA TAC ACA CCC TTT GGA AGT-3′ and 5′-AGC TCA ATG CAT GTA CAG AAT CCC CGG TTA-3′; product size, 382 bp) or villin as a control (5′-CAG CTA GTG AAC AAG CCT GTA GAG GAG CTC-3′ and 5′-GCC ACA GAA GTT TGT GCT CAT AGG CAC ATC-3′; product size, 303 bp) and 41.6 μl of RNase-free dH_2O. The reaction mixtures were heated to 95°C and then allowed to anneal, followed by addition of 2.5 U *Taq* DNA polymerase. PCR was then carried out in 40 thermal cycles consisting of 95°C for 30 s, 60°C for 30 s, and 65°C for 2 min. After completing all cycles, a 10-min extension step at 65°C was performed and the PCR products were then electrophoresed on agarose gels, stained with ethidium bromide and analyzed by densitometric scanning of the gel images.

Western Blotting

Transfected HT-29, Intestine-407, or COS-7 cells were lysed directly in 2% SDS, 5% β-mercaptoethanol, 125 mM Tris-HCl, pH 6.8, and 20% glycerol, and 100 μg of cellular protein were run on 5–15% gradient SDS/polyacrylamide gels. After electrophoretic fractionation, proteins were electrotransferred to Immobilon-P membranes (Millipore Corp., Bedford, MA) using a Transblot apparatus in 25 mM Tris-HCl, pH 7.4, 192 mM glycine, 0.01% SDS, and 20% methanol. The membrane was then blocked by incubation for 3 h with 3% blotto (3% dry milk, 10 mM Tris-HCl, pH 7.5, 150 mM NaCl). Immunodetection of bound human CYP3A4 protein was then performed using the monoclonal anti-hCYP3A4, MAB-3A (BD Gentest, Woburn, MA), while detection of VDR was accomplished using the anti-VDR monoclonal antibody, 9A7γ [Pike, 1984]. After the first antibody treatment (1:2,000 dilution for CYP3A4, 1:10,000 for VDR), the Immobilon-P membrane was washed and treated at room temperature for 1 h with goat anti-mouse IgG (or anti-rat for VDR) conjugated to biotin followed by four 15 min washes. A 5 ml mixture of biotinylated alkaline phosphatase and neutravidin (Pierce, Rockford, IL; in a ratio of 1:4) was pre-incubated for 45 min at 22°C in 1% blotto. The mixture was diluted to 30 ml with 1% blotto and added to the membrane for a 2 h incubation with rocking at room temperature and then was washed four more times, followed by a fifth wash with biotin blot buffer (0.1 M Tris-HCl, pH 9.5, 0.1 M NaCl, 2 mM $MgCl_2$, 0.05% Triton X-100). Finally, the blot was exposed to color reagent containing 50 μg/ml of 5-bromo-4-chloro-3-indolyl-phosphate and 100 μg/ml of 4-nitroblue tetrazolium chloride. The color reaction was stopped by washing with distilled water.

Preparation of Cellular Extracts and Gel Mobility Shift Assays

The hVDR and RXRα proteins utilized for gel mobility shift assays were obtained from either whole cell extracts of transfected COS-7 or HT-29 cells. Cells (800,000 cells/60-mm plate) were transfected with 0.2 μg of WT pSG5-hVDR expression plasmid. Sixteen-hours post-transfection, the cells were washed and refed in DMEM. After 24 h, the cells were washed twice with phosphate buffered saline (136 mM NaCl, 26 mM KCl, 8 mM Na_2HPO_4, 1.5 mM KH_2PO_4, pH 7.2), and scraped into 200 μl of KETZD-0.3 buffer (10 mM Tris-HCl, pH 7.6, 1 mM EDTA, 0.3 mM $ZnCl_2$, 0.3 M KCl, 10% glycerol, 1 mM DTT, 0.1 mM phenylmethylsulfonyl fluoride, 15 μg/ml aprotinin, 1 μg/ml leupeptin, 1 μg/ml

pepstatin A). After sonication, samples were centrifuged at 16,000*g* for 15 min at 4°C and the hVDR-containing supernatant was utilized in electrophoretic mobility shift assays as described previously [Thompson et al., 1998]. Briefly, 5 μl of cell lysate were incubated with ethanol vehicle or 10^{-4}–10^{-7} M ligands in DNA-binding buffer (10 mM Tris-HCl, pH 7.6, 150 mM KCl, 1 mg/ml acetylated BSA, 50 μg/ml poly [deoxyinosinic-deoxycytidylic acid]) for 45 min at 22°C followed by the addition of 0.5 ng of [^{32}P]-labeled double stranded oligomers containing the putative VDRE sequence (see Fig. 2 for designations and DNA sequences) and incubation for an another 30 min. Some reactions also included 1 μg of either an anti-VDR monoclonal antibody (9A7) known to specifically inhibit VDR-RXR binding to the VDRE under the conditions employed in this assay [Thompson et al., 1998], or a partially purified fragment of SRC-1 containing three LXXLL domains. Electrophoresis and autoradiography conditions were as described previously [Nakajima et al., 1994].

Mammalian Two-Hybrid Assays

Protein-protein interactions between VDR, retinoic acid receptor α (RARα), and a panel of known nuclear receptor co-modulators were examined through use of a mammalian two-hybrid system. The mammalian two-hybrid vectors pM (BD Biosciences, San Jose, CA), pCMVBD, and pCMVAD (Stratagene) were made compatible with the gateway cloning system, through insertion of gateway reading frame cassette C.1 (Invitrogen, Carlsbad, CA) into the multiple cloning site of each plasmid. DNA fragments coding for SMRT (aa 2004–2448), SRC-1 (aa 552–872), SRC-2 (aa 640–991), SRC-3 (aa 615–785), VDR (aa 96–427), RARα (aa 111–462), and RXRα (aa 197–461) were amplified by PCR from a human fetal brain cDNA library (Invitrogen). The respective gene-specific forward and reverse primers contained the 5′-terminal extensions *att*B1 (5′-GGG GAC AAG TTT GTA CAA AAA AGC AGG CT-3′) and *att*B2 (5′-GGG GAC CAC TTT GTA CAA GAA AGC TGG GT-3′). Entry clones for each gene fragment were created by insertion of purified PCR product into the donor vector pDONR201 using the BP clonase recombination reaction (Invitrogen). The respective entry clones were in turn inserted into the appropriate gateway modified mammalian two-hybrid plasmid by LR clonase reaction (Invitrogen). Constructs were subjected to DNA sequencing to confirm identity and reading frame for each gene insert.

Two-hybrid assays were performed using Chinese hamster ovary (CHO) cells maintained at 37°C in 5% CO_2 in DMEM nutrient mixture F12 HAM (Sigma) supplemented with 10% FBS and 100 U/ml penicillin and 100 μg/ml streptomycin. Co-transfection experiments were performed using Lipofectamine 2000 (Invitrogen), with prey (pCMVAD) and bait (pCMVBD or pM) fusion constructs in combination with the reporter pFLUC and the pRL-TK internal control. The total amount of DNA used per well was 150 ng. Cells were then treated with ligand and incubated for 24 h at 37°C. After ligand exposure, cells were harvested and luciferase assays were performed with the dual-luciferase reporter assay as described by the manufacturer's (Promega) manual. Transfection data were normalized to the RL control and expressed as a mean of relative light units from triplicate assays ± the standard deviations (SDs).

GST Pulldown Assays

WT hVDR cDNA was cloned into the EcoRI site of the glutathione-S-transferase (GST) fusion protein vector, pGEX-4T (Pharmacia Biotech, Uppsala, Sweden), to create GST-hVDR. The GST fusion construct was transformed into *E. coli* (strain BL21). GST alone was expressed from pGEX-4T in *E. coli* strain DH5α and linked to glutathione-Sepharose beads to serve as a control for background protein association. For GST pulldown assays, expression plasmids for VDR interacting proteins (VIPs) (1.0 μg each) were used to generate [^{35}S] methionine-labeled VIPs by in vitro transcription/translation (TNT Coupled Reticulocyte lysate kit, Promega Corp., Madison, WI). As described in detail elsewhere [Jurutka et al., 2000], GST-control and GST-hVDR Sepharose beads (25 μl each) were incubated in KETZD-0.15 M buffer (10 mM Tris-HCl, pH 7.6, 1 mM EDTA, 0.3 mM $ZnCl_2$, 1 mM dithiothreitol, 10% glycerol, 200 ng/ml pefabloc SC (Roche Molecular Biochemicals, Indianapolis, IN), 15 μg/ml aprotinin, 1 μg/ml leupeptin, and 1 μg/ml pepstatin A, plus 0.15 M KCl, 0.1% Tween-20, and 1 mg/ml BSA) at 4°C for 1.5 h on a rocking platform in the absence or presence of lipophilic ligands and/or VDREs: 1,25$(OH)_2D_3$ (10^{-6} M), LCA (10^{-4} M), 3-keto-lithocholic acid (10^{-4} M), cholic acid (10^{-4} M), or 10^{-7} M CYP3A4 XDR3

VDRE. Next, the desired [^{35}S]-labeled protein(s) was incubated with the beads for 30 min at 4°C. The beads were then washed four times with KETZD-0.15 to remove unbound protein(s). The bound proteins were extracted from the beads into loading buffer (4% SDS, 10% β-mercaptoethanol, 125 mM Tris-HCL, pH 6.8, 20% glycerol), boiled 3 min, and separated by gradient (5–20%) SDS–PAGE and visualized by autoradiography. The amount of extract analyzed as input was 5% of the amount used in pulldown reactions.

Transcriptional Interference Assay Employing a Glucocorticoid Receptor-Mediated Transcription System

COS-7 cells (750,000 cells/60-mm plate) were transfected by the calcium phosphate-DNA coprecipitation method as described previously [Jurutka et al., 1993] with 0.5 μg of WT mGR expression plasmid (pSG5-mGR) [MacDonald et al., 1993] and 0.5 μg pSG5-hVDR expression plasmid [Hsieh et al., 1991] along with a reporter vector containing either the glucocorticoid responsive element (GRE) derived from the long terminal repeat of the mouse mammary tumor virus [Scheidereit et al., 1983] or the (CYP3A4 XDR3)^2 VDRE linked upstream of the thymidine kinase promoter driving the expression of the human GH gene. Some cells received 0.5 μg of mutant hVDR (E420A) and/or an expression plasmid for the SRC-1 or GRIP1 coactivators. The pTZ18U plasmid was used as carrier to adjust total DNA to 20 μg/plate. Following transfection, cells were treated for 24 h with 10^{-7} M 1,25(OH)$_2$D$_3$, 10^{-6} M dexamethasone, 10^{-4} M LCA, or ethanol vehicle. Media were then assayed for human GH by radioimmunoassay using a commercial kit (Nichols Institute).

RESULTS

LCA and 1,25(OH)$_2$D$_3$ Induce CYP3A4 in Human Colon Cancer Cells

The first goal of this study was to test directly the role of LCA in regulating CYP3A4 in human enteric tract cells, and to analyze the numerous putative VDREs in the CYP3A4 promoter. HT-29 human colon cancer cells were employed initially in order to evaluate the effect of various nuclear receptor ligand treatments on the expression of the endogenous *CYP3A4* gene in intestine. As shown in Figure 1A, 1,25(OH)$_2$D$_3$

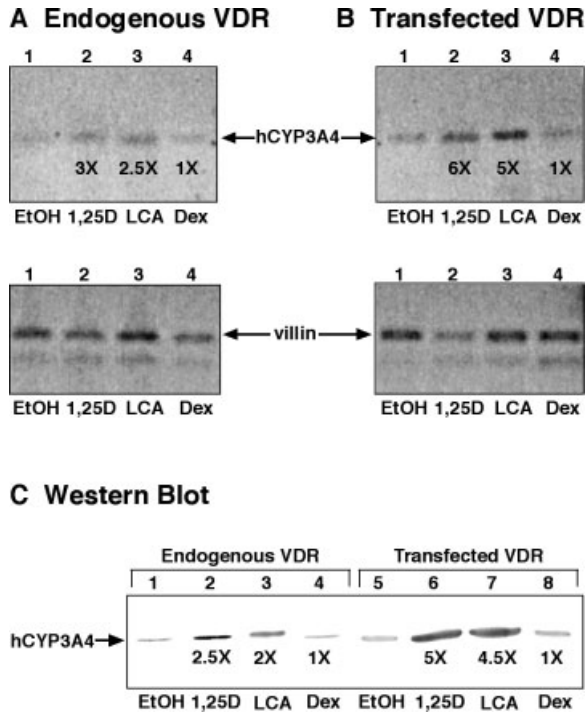

Fig. 1. Induction of CYP3A4 by 1,25(OH)$_2$D$_3$ and LCA in human colon cancer cells. **A**: HT-29 colon adenocarcinoma cells were mock transfected with carrier DNA and treated with ethanol vehicle (EtOH, **lane 1**), 10^{-8} M 1,25(OH)$_2$D$_3$ (1,25D, **lane 2**), 10^{-4} M lithocholic acid (LCA, **lane 3**), or 10^{-5} M dexamethasone (Dex, **lane 4**) for 24 h. Cellular lysates were prepared, followed by isolation of poly(A)$^+$ RNA that was then subjected to semi-quantitative RT-PCR analysis. The intensity of each band was quantitated by densitometric scanning and the fold induction of the human CYP3A4 transcript in response to hormone treatment is shown after normalization to the level of villin expression (lower blot). **B**: Analysis of HT-29 cells treated as in (A), except the cells were transfected with an expression vector encoding the full-length human VDR (hVDR). **C**: Parallel extracts containing 100 μg each of protein from cells treated as in (A) and (B) were fractionated on 5–15% gradient SDS/polyacrylamide gels followed by Western blotting employing a monoclonal antibody directed against human CYP3A4.

and LCA elicit an approximate two- to three-fold induction of hCYP3A4 mRNA at 24 h as assessed by RT-PCR. Dexamethasone, the synthetic glucocorticoid ligand that binds to PXR and induces CYP3A4 at micromolar concentrations, did not induce CYP3A4 mRNA in HT-29 colon cells as it does in liver [Luo et al., 2002; Kliewer, 2003]. Thus, although PXR and VDR are closely related in sequence [Kliewer et al., 1998] and structure [Watkins et al., 2001], and PXR has some affinity for LCA [Staudinger et al., 2001], the actions of LCA in HT-29 cells are likely mediated mainly by VDR. Consistent with this observation, overexpression of VDR in HT-29 cells amplifies the induction of CYP3A4 mRNA

by $1,25(OH)_2D_3$ and LCA to six- and five-fold, respectively (Fig. 1B). As illustrated in Figure 1C, immunoblot analysis verifies that $1,25(OH)_2D_3$ or LCA treatment increases CYP3A4 protein concentrations in HT-29 cells in a manner quantitatively comparable to the augmentation of mRNA levels, implying that functional CYP3A4 enzyme is produced in response to either ligand. Similar qualitative results for CYP3A4 induction were obtained when human embryonic epithelial cells derived from the jejunum/ileum (Intestine-407) were treated with $1,25(OH)_2D_3$ or LCA (data not shown), demonstrating that stimulation of CYP3A4 expression by $1,25(OH)_2D_3$, and potentially by LCA, occurs in cells from both the small and large intestine.

Identification and Evaluation of DR3 and ER6 VDREs in the Human CYP3A4 Promoter

We then scanned the 5′-flanking region of human CYP3A4 for putative VDREs that likely mediate the effect of $1,25(OH)_2D_3$ or LCA on the expression of this gene by comparing its promoter region to that of well-characterized genes regulated by $1,25(OH)_2D_3$, including the bone remodeling proteins, osteopontin, and osteocalcin, expressed in osteoblasts, and CYP24, the cytochrome P450 enzyme responsible for vitamin D catabolism [Haussler et al., 1998]. All of these genes contain one or more classic VDREs consisting of an imperfect DR3-type element of tandem AGGTCA-like repeats, with the 5′ half-site potentially occupied by RXR and the 3′ half-element binding to VDR. Therefore, the criteria for CYP3A4 VDRE selection included either the presence of classical DR3-like elements, or novel ER6 elements that are known targets for PXR, which also regulates the transcription of CYP3A4 [Lehmann et al., 1998; Staudinger et al., 2001; Xie et al., 2001]. Figure 2A shows the rat osteocalcin promoter that contains the typical DR3 element located within the first 500 base pairs of the promoter (PDR3) and Figure 2B illustrates the rat *CYP24* gene that possesses dual antisense DR3s (XDR3 and PDR3) that are positioned within 300 base pairs of the start site for transcription. In sharp contrast, the human CYP3A4 promoter region is quite complex, containing several postulated VDREs of the DR3 and ER6 type as detailed in Figure 2D. In addition to hCYP3A4, we also examined the promoter sequence of rat CYP3A23, which is the major inducible *CYP* gene in rat liver and intestine [Huss et al., 1996;

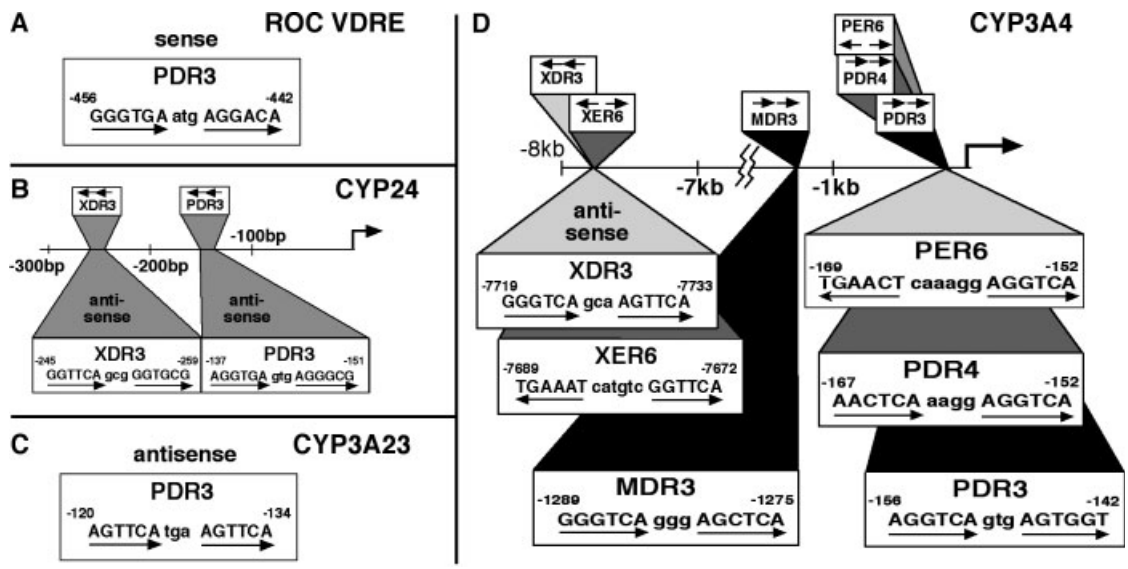

Fig. 2. Schematic representation of known or putative VDREs in rat osteocalcin and cytochrome P450 (*CYP*) genes that were evaluated in this study. The sequences of previously known VDREs, all of the DR3 type, and their positions relative to the transcriptional start site of three VDR-regulated genes are shown at **left**. These VDREs include: **A**: rat osteocalcin (ROC VDRE); **B**: two antisense rat 24-hydroxylase (CYP24) elements; and **C**: an antisense rat cytochrome P450 3A23 (CYP3A23) element. **D**: Several recently discovered [Thummel et al., 2001; Thompson et al., 2002] and putative VDREs from the human *CYP3A4* gene promoter region are illustrated at **right**. CYP3A4 elements furthest upstream include the antisense distal direct repeat-3 (XDR3) and a potential distal everted repeat-6 (XER6), as well as a putative medial direct repeat-3 (MDR3). Elements closest to the TATA box consist of a proximal everted repeat-6 (PER6), a potential proximal direct repeat-4 (PDR4) which is contained within the sequence of the PER6, and a prospective proximal direct repeat-3 (PDR3).

Huss and Kasper, 2000], and located a perfect DR3 as a candidate VDRE (Fig. 2C).

Biochemical evaluation of these candidate hCYP3A4 VDREs, as well as the perfect DR3 in the rat *CYP3A23* gene, was first carried out employing transcriptional activation studies with an hVDR expression vector and the various VDRE-linked GH reporter gene constructs in cotransfected human cells derived from small intestine (Intestine-407) and from colon cancer (HT-29). As depicted in Figure 3, transcriptional activation by $1,25(OH)_2D_3$ and LCA was investigated using reporter constructs containing dual copies of each CYP VDRE, with a four-copy ROC and a two-copy distal rat CYP24 (24 XDR3) [Zierold et al., 1994] VDRE-reporter vector serving as positive controls. Dexamethasone, a PXR ligand that can induce CYP3A4 expression in liver [Staudinger et al., 2001], was utilized to probe possible involvement of PXR in CYP3A4 induction in intestinal cells through DR3/ER6 VDREs, and displayed no stimulation at 10^{-5} M from any of the tested VDRE reporter constructs (Fig. 3, labeled "+X"). The overall pattern of transactivation by $1,25(OH)_2D_3$ from the various candidate VDREs was similar in both intestinal cell lines, and demonstrated that the CYP3A23 DR3 and especially the CYP3A4 XDR3 are, on a per copy basis, significantly more potent than the ROC VDRE (Fig. 3A and B, top panels). Interestingly, on a per copy basis, the CYP3A4 proximal ER6 element (PER6) exhibited approximately the same efficacy as the ROC DR3 VDRE (Fig. 3A,B, top panels). The PDR4 element imbedded within the PER6 (see Fig. 2D) does not contribute to the activity of the PER6 VDRE because the former is incapable of driving $1,25(OH)_2D_3$-stimulated transcription (Fig. 3, lower panels). The pattern of LCA-mediated transactivation is also similar in the two cell lines, and a consistent observation is that this bile acid ligand, while inducing a significant level of reporter gene activation, is less potent than the $1,25(OH)_2D_3$ hormone in Intestine-407 cells (an average of 60% of the activity achieved with $1,25(OH)_2D_3$). This is also true in the HT-29 colon cancer cellular background, although, in this context, LCA appears to be almost as effective as $1,25(OH)_2D_3$ when select VDREs are utilized

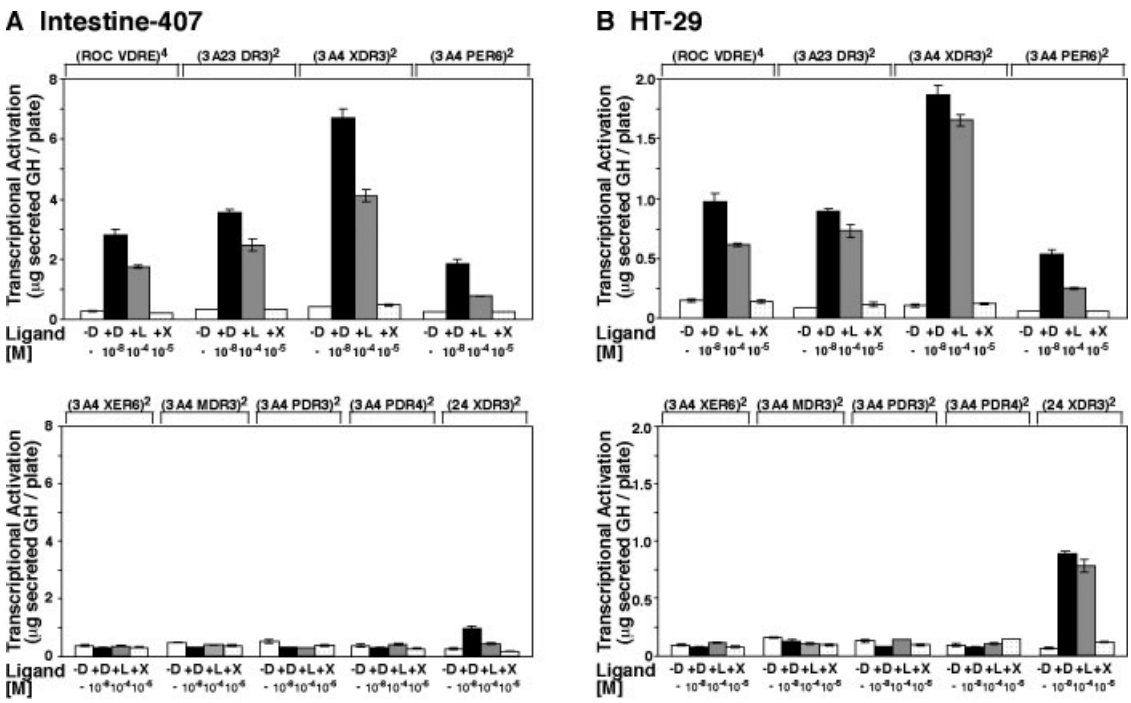

Fig. 3. Evaluation of $1,25(OH)_2D_3$ and LCA responsiveness of selected VDREs in transfected intestinal cells. **A**: Intestine-407 cells were cotransfected with 10 µg of a reporter plasmid containing four copies of the rat osteocalcin VDRE linked to the human GH gene (ROC VDRE)^4, or with reporter vectors containing two copies of the indicated CYP VDREs (see Fig. 2 for designations and sequences), 0.3 µg of pSG5-hVDR expression plasmid, and pTZ18U carrier DNA. Cells were treated for 24 h post-transfection with 10^{-8} M $1,25(OH)_2D_3$ (+D), 10^{-4} M LCA (+L), 10^{-5} M dexamethasone (+X), or ethanol vehicle (−D). **B**: HT-29 cells were transfected as in (A), except that 2.0 µg of pSG5-hVDR expression plasmid were used.

(Fig. 3B, 3A23 DR3, 3A4 XDR3 and 24 XDR3). In addition, all candidate VDREs tested that do not display transcriptional activity with $1,25(OH)_2D_3$ are also inactive when assayed with LCA. Taken together, the results indicate that the *CYP3A4* gene promoter contains a minimum of two biologically relevant VDREs, the XDR3 and PER6, which constitute distinctly different DNA motifs, and are both responsive to $1,25(OH)_2D_3$ and LCA.

VDR Activation Is Selective for LCA and 3-KetoLCA Among Bile Acids

We next assessed the selectivity of bile acid activation of VDR and also the ability of LCA to activate both exogenous and endogenous VDR in several different cellular contexts that represent classic $1,25(OH)_2D_3$ target tissues, including kidney, bone, and intestinal cells. In these experiments, the well-established ROC and rat CYP24 VDREs were employed to probe transcriptional activation of transfected cells. In Figure 4A, COS-7 monkey kidney cells were cotransfected with a reporter vector containing four copies of the ROC or CYP24 proximal [Ohyama et al., 1994] VDRE and an expression vector for hVDR. The results reveal that, at 10^{-4} M, LCA (+L) and its 3-keto derivative (+K) can significantly enhance VDR-mediated transcription, up to 70% of that observed with $1,25(OH)_2D_3$. Importantly, other bile acids including cholate (+C), deoxycholate (+O), and ursocholate (+U), which are structurally related to LCA, do not activate transcription of the VDRE-linked reporter gene in this system. Similar results were obtained in human embryonic kidney cells (HEK-293), which contain endogenous receptor and therefore were not supplemented, as was done in Figure 4A, with a VDR expression vector. LCA and $1,25(OH)_2D_3$, but not the primary bile acid, cholate, possessed significant activity at 10^{-4} M, but a lower concentration of LCA (10^{-6} M) did not elicit transactivation (Fig. 4B). Two different rat osteoblast-like osteosarcoma (ROS) cell lines were tested next to further probe the activity of LCA. The ROS 2/3 line does not possess significant endogenous VDR, so these cells were transfected with an expression vector for hVDR along with the four-copy ROC VDRE and treated with the indicated ligands (Fig. 4C). The results specify that LCA, but not cholic acid, is a potent VDR activator in these cells. In contrast, when ROS 17/2.8 cells, which contain abundant

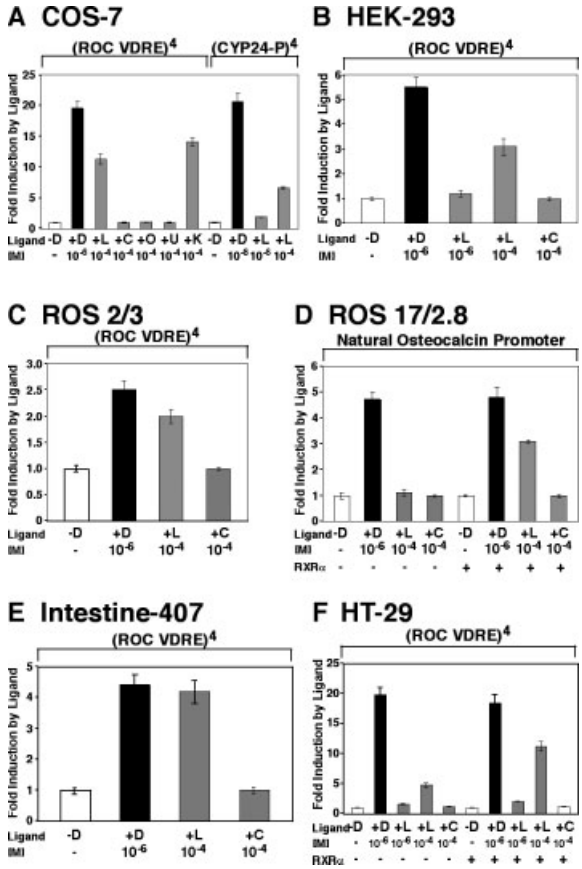

Fig. 4. Assessment of $1,25(OH)_2D_3$- and bile acid-stimulated transactivation mediated by VDR in kidney, bone, and intestinal cells. All cultures except those shown in **panel D** were transfected with a GH reporter construct under the control of four copies of the indicated VDRE. Added $1,25(OH)_2D_3$ is denoted +D, bile acids tested include lithocholate (+L), 3-ketolithocholate (+K), cholate (+C), deoxycholate (+O), and ursocholate (+U). **A**: Kidney-derived COS-7 cells were also transfected with a VDR expression plasmid in addition to the GH reporter. ROC is the VDRE from the rat osteocalcin gene. CYP24-P is the proximal VDRE from the rat 24-hydroxylase gene. **B**: Results with human embryonic kidney cell line HEK-293 (contains endogenous VDR). **C**: The VDR-deficient rat osteosarcoma line ROS 2/3 was transfected with a VDR expression plasmid in addition to the reporter construct. **D**: Results with ROS 17/2.8 cells (endogenous VDR) and the bone-specific natural promoter (approximately 1,100 bp of upstream sequence) from the rat osteocalcin gene. Some plates also received an expression plasmid for human RXRα. **E**: The human embryonic line Intestine-407 was transfected with a VDR expression plasmid in addition to the reporter construct. **F**: Results with the human colon adenocarcinoma line HT-29 (endogenous VDR ± exogenous human RXRα).

levels of endogenous VDR, were analyzed using a reporter construct containing 1,100 bp of the rat osteocalcin natural promoter linked to the GH reporter gene [Terpening et al., 1991], only $1,25(OH)_2D_3$ produced a significant level of GH induction (Fig. 4D). The overexpression of

RXRα, the heterodimeric DNA binding partner for VDR, was required for LCA-mediated transcription to occur in ROS 17/2.8 cells (Fig. 4D, right). A similar requirement for RXRα in the presence of LCA was also observed in HT-29 colon cancer cells employing endogenous VDR and the ROC VDRE reporter gene, although in these cells LCA displays modest activity in the absence of additional RXR (Fig. 4F), but only at the higher concentration of LCA (10^{-4} M). In contrast, LCA appears to be as effective as $1,25(OH)_2D_3$ in Intestine-407 cells transfected with VDR and ROC VDRE (Fig. 4E); however, this result is dependent on the efficiency of the transfection and is not observed when transfection efficacy and fold-stimulation by $1,25(OH)_2D_3$ are elevated as in Figure 3A (ROC VDRE). The collective results presented in Figure 4 suggest that VDR-mediated transactivation is selective for $1,25(OH)_2D_3$ and the bile acid LCA, as well as its 3-keto metabolite. LCA, at a dose of 10^{-4} M, can activate both endogenous and cotransfected VDR in several different cell lines that encompass classic $1,25(OH)_2D_3$ target tissues. In certain cellular milieus, LCA is nearly as effective as $1,25(OH)_2D_3$ (Fig. 4C,E), whereas in other cell types overexpression of RXR is required for significant LCA-stimulated transcription (Fig. 4D,F).

LCA Liganding of VDR Generates VDR-RXR Heterodimers

Given the observation that RXR overexpression can, in some cases, increase sensitivity of VDR to LCA, we next probed the ability of LCA to induce VDR-RXR heterodimerization and facilitate DNA binding by utilizing gel mobility shift analysis. COS-7 cells were transfected with an expression vector for hVDR and used to generate cell extracts that were incubated with the ROC VDRE, which was employed as a positive control. ROC VDRE displays robust $1,25(OH)_2D_3$-dependent binding to VDR-RXR that is strongly inhibited by the 9A7 VDR antibody (Fig. 5A, lanes 1–3). LCA can also elicit heterodimerization and VDRE binding at concentrations as low as 10^{-5} M (lanes 4–5), albeit the binding is slightly weaker than that observed with $1,25(OH)_2D_3$. Inclusion of the 9A7 VDR antibody effectively reduces VDRE binding (lane 6). Incubation with cholic acid does not stimulate a VDR–RXR complex above basal levels (lane 7). Further biochemical

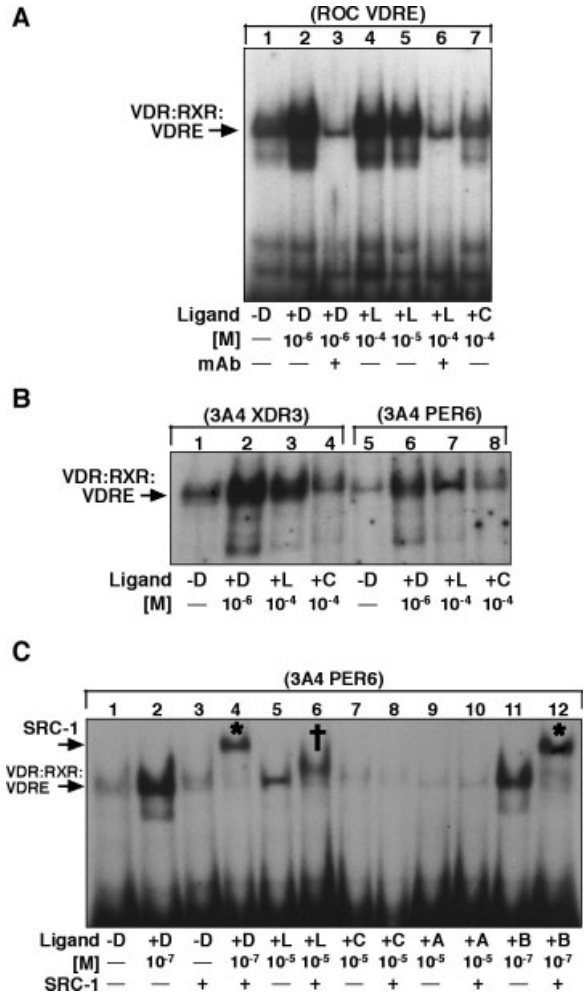

Fig. 5. Ligand-dependent gel mobility shift assay analysis of candidate CYP VDREs. **A**: A gel shift assay was performed using whole cell extracts from COS-7 cells transfected with 0.2 μg of expression vector for WT hVDR. Employing the established DR3 VDRE from the *ROC* gene, **lanes 1** and **2** indicate DNA complexes formed by VDR in combination with RXR in the absence and presence of 10^{-6} M $1,25(OH)_2D_3$ (+D), respectively, while **lane 3** shows the effect of the presence of the VDR specific monoclonal antibody, 9A7 (1 μg), which inhibits DNA binding. **Lanes 4–6** represent a similar pattern of treatment with two different concentrations of LCA (+L), whereas **lane 7** includes treatment with cholic acid as a negative control. **B**: Additional VDREs were analyzed as in (A), except that extracts from transfected HT-29 cells were used. Probes include the distal DR3 (3A4 XDR3; **lanes 1–4**) and proximal everted repeat-6 (3A4 PER6; **lanes 5–8**) from the human *CYP3A4* gene. **C**: Employing PER6 and HT-29 extracts as in **panel B**, an SRC-1 fragment containing three LXXLL domains was included in the indicated binding reactions. A supershifted complex (designated by *) was observed in the presence of $1,25(OH)_2D_3$ (**lane 4**) and the vitamin D agonist EB1089 (+B; **lane 12**), a partial supershift (designated by †) was detected with LCA (+L; **lane 6**), and no supershift was present using cholic acid (+C) or vitamin D_3 (+A) (**lanes 8** and **10**, respectively).

evaluation of the two identified hCYP3A4 VDREs, namely XDR3 and PER6 (Fig. 2B), was carried out by gel mobility shift analysis, but employing cellular extracts from hVDR transfected HT-29 cells (Fig. 5B). Both VDREs display strong $1,25(OH)_2D_3$- and LCA-mediated binding to the VDR-RXR heterodimer, with the XDR3 element possessing more potent association compared to the PER6 (Fig. 5B, lanes 2–3 and 6–7). Also, as observed with the ROC VDRE and COS-7 cell extracts (Fig. 5A), LCA-stimulated heterodimerization of VDR and RXR is slightly weaker than that generated by $1,25(OH)_2D_3$, especially when employing the PER6 VDRE (Fig. 5B, lanes 6–7). We utilized this somewhat differential binding of $1,25(OH)_2D_3$-VDR versus LCA-VDR to the PER6 element to investigate the ability of liganded VDR-RXR to interact with an SRC-1 coactivator fragment containing three LXXLL interaction domains. Incubation of HT-29 extracts with $1,25(OH)_2D_3$ or LCA results in the formation of the VDR-RXR-VDRE complex (Fig. 5C, lanes 2 and 5). Upon addition of the SRC-1 fragment, a VDR-RXR-VDRE-SRC supershifted complex is observed (indicated by *) that is strictly dependent on the presence of $1,25(OH)_2D_3$ or the transcriptionally active $1,25(OH)_2D_3$ analog, EB1089 (+B; compare lanes 2 and 4 with 11–12). Inclusion of LCA in the reaction mixture with SRC-1 results only in a partial supershifted complex (lane 6, indicated by †), while cholic acid (+C) or vitamin D_3 (+A) do not generate any shifted complex above basal (−D) levels, as expected. Taken together, these results indicate that the distal DR3 (XDR3) and proximal ER6 (PER6) exhibit strong, $1,25(OH)_2D_3$- and LCA-enhanced VDR-RXR binding, in vitro, similar to that displayed by the rat osteocalcin VDRE. There is a differential interaction of SRC-1 and RXR with LCA-VDR bound to DNA compared to that observed with $1,25(OH)_2D_3$- or analog-liganded VDR. This suggests an attenuated affinity of SRC-1 and RXR for LCA-VDR in this setting, perhaps the result of an altered conformation of VDR when bound to its bile acid ligand.

LCA Liganded VDR Is a Less Effective Recruiter of Comodulators in Intact Cells Than Is $1,25(OH)_2D_3$-VDR

To assess the capacity of $1,25(OH)_2D_3$- and LCA-VDR to recruit protein partners within the context of intact cells, the ability of $1,25(OH)_2D_3$- and LCA-bound VDR to interact with a number of known nuclear receptor comodulatory proteins, including RXR and SRC, was monitored through use of a mammalian two-hybrid assay system in CHO cells. Figure 6A demonstrates that VDR expressed as "bait", in combination with the empty "prey" vector (bdVDR-ad) results in a significant (145-fold) induction of the pFR-Luc reporter vector upon treatment with $1,25(OH)_2D_3$ but not with the RXR ligand 9-*cis* retinoic acid (RA). This activation is likely due to recruitment by liganded VDR of endogenous cellular RXR and coactivators to the GAL4-DBD-VDR fusion construct to form an "active" VDR-RXR heterodimer. Addition of LCA results in a significant (twofold; not visible in Fig. 6A), albeit reduced activation of the reporter. The combination of VDR as "prey" with the VDR "bait" construct (bdVDR-VDRad) did not result in an enhancement of the reporter signal (over that obtained with bdVDR-ad) upon dosage with any of the ligands, indicating that neither the $1,25(OH)_2D_3$ nor LCA ligand can promote formation of a VDR-VDR homodimer. Expression of RXR (bdRXR-ad) produced an activating reporter signal only in the presence of its cognate ligand, 9-*cis* RA (24-fold induction), likely as a result of dimerization between the RXR fusion construct and cellular RXR/coactivators. When RXR was expressed as "bait" with the VDR "prey" vector (bdRXR-VDRad), both $1,25(OH)_2D_3$ (273-fold) and LCA (53-fold) treatment of the transfected cells resulted in a significant increase in the reporter signal, indicating that both ligands, upon binding to VDR, promote recruitment of RXR to form the heterodimeric complex.

The ability of $1,25(OH)_2D_3$ and LCA to promote interaction between VDR and members of the p160 family of coactivators is represented in panel B (Fig. 6). Treatment of transfected cells with $1,25(OH)_2D_3$ was observed to promote the formation of complexes between VDR and SRC-1, -2 and -3 (also known as NCoA-1, GRIP1/TIF2/NCoA-2, and pCIP/RAC3/ACTR/TRAM-1/AIB1, respectively [McKenna et al., 1999a; McKenna and O'Malley, 2002]). In contrast, neither LCA nor the PXR ligand, clotrimazole, were able to induce any significant interaction between VDR and the p160 coactivators, at least in this system. We then compared the profile of ligand-dependent coactivator recruitment exhibited by RARα with that produced by VDR. The results in panel C illustrate that RARα recruits

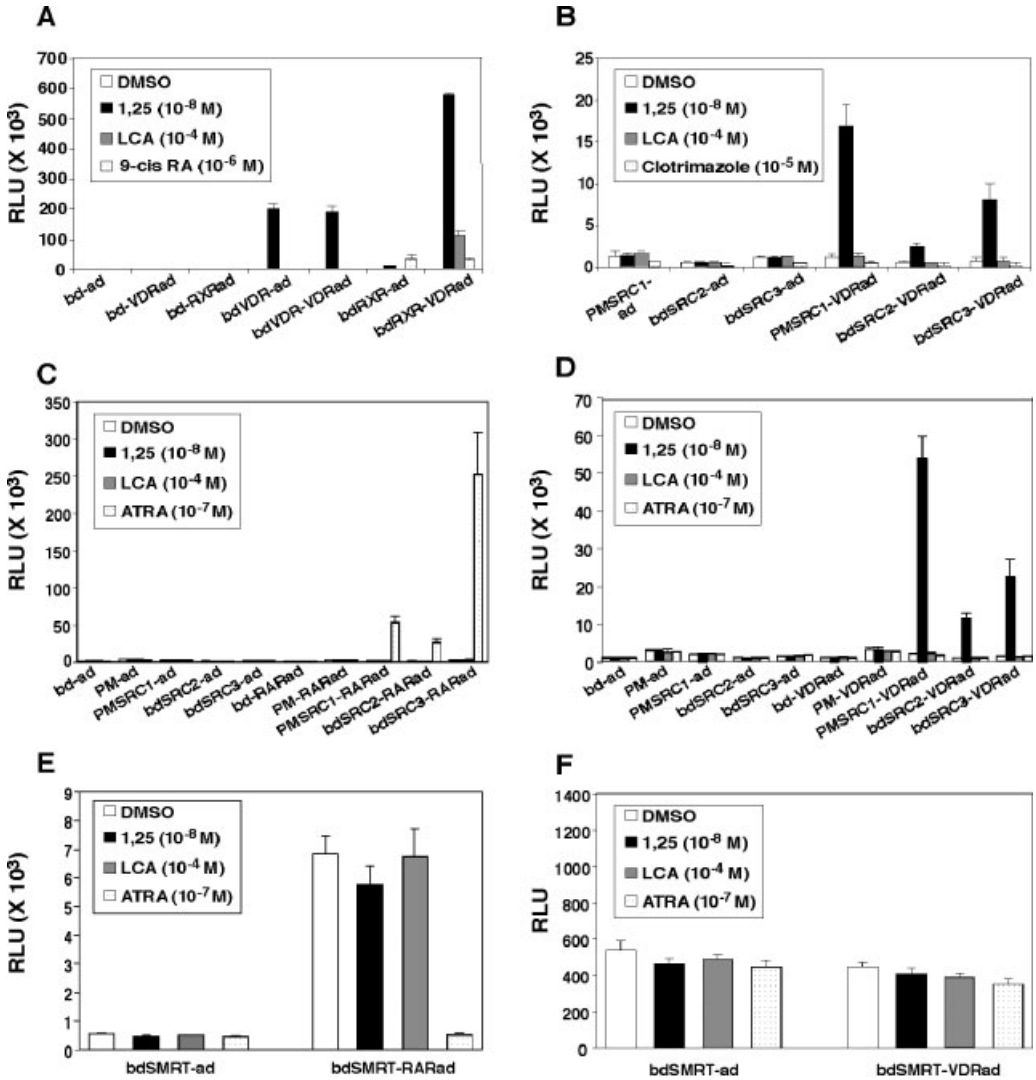

Fig. 6. Analysis of $1,25(OH)_2D_3$- and LCA-VDR utilizing the mammalian two-hybrid system to probe for protein–protein interactions. The ligands employed were $1,25(OH)_2D_3$ (1,25), lithocholic acid (LCA), all-*trans* retinoic acid (ATRA), 9-*cis* retinoic acid (9-cis RA), and clotrimazole to generate interactions between VDR and a panel of known nuclear receptor comodulatory proteins. CHO cells were cotransfected with prey (ad) and/or bait (PM or bd) fusion constructs in combination with the pFR-Luc reporter vector and the pRL-TK control plasmid. Cells were incubated for 24 h in the presence of ligand at the indicated concentrations followed by measurement of luciferase. After normalization for transfection efficiency, results were expressed as relative light units (RLU) per well. **A**: LCA and $1,25(OH)_2D_3$ can induce formation of the VDR-RXR heterodimer. RXRα and VDR are shown to interact (bdRXR–VDRad) in the presence of LCA and $1,25(OH)_2D_3$, but not 9-*cis* RA. Comparison of the RLU values observed using bdVDR-ad and bdVDR-VDRad indicate that none of the tested ligands were able to induce VDR homodimerization above background. The remaining data sets represent controls. **B**: $1,25(OH)_2D_3$, but neither LCA nor the PXR ligand clotrimazole, can promote significant interaction between VDR and SRC1, SRC2, or SRC3. **C**: Retinoic acid receptor interacts with SRC1, SRC2, and SRC3 in the presence of its cognate ligand, ATRA, but not in the presence of $1,25(OH)_2D_3$ or LCA. **D**: $1,25(OH)_2D_3$, but neither LCA nor ATRA, can promote interaction between VDR and the tested p160 coactivators. **E**: The transcriptional corepressor SMRT constitutively interacts with RAR (compare bdSMRT-ad with bdSMRT-RARad). SMRT is released from RAR only upon binding of ATRA but not in the presence of $1,25(OH)_2D_3$ or LCA. **F**: SMRT does not interact with VDR either constitutively or in the presence of any tested ligand (note difference in RLU scale between panels E and F).

SRC-1, -2 and -3 only upon binding its cognate ligand, all-*trans* RA (ATRA) and not when exposed to $1,25(OH)_2D_3$ or LCA, thus emphasizing the ligand specificity of the assay system. A complementary ligand specificity is illustrated for VDR in panel D, again highlighting that $1,25(OH)_2D_3$ promotes coactivator recruitment by VDR, but LCA and ATRA are incapable of causing significant interaction with coactivators. The data also reveal that VDR and RAR

exhibit a different pattern of p160 coactivator recruitment, with VDR interacting most avidly with SRC-1 (panels B and D) and RARα displaying a preference for SRC-3 (panel C).

We then examined the impact of LCA, $1,25(OH)_2D_3$ and ATRA on interaction of VDR or RARα with the corepressor SMRT. Panel 6E illustrates that co-transfection of the SMRT bait and RARα prey constructs results in a strong activation of reporter activity as a result of the constitutive interaction between unliganded RARα and SMRT. This association is disrupted only in the presence of ATRA and is unaffected by treatment of cells with $1,25(OH)_2D_3$ or LCA. In contrast, panel F reveals that no interaction between VDR and SMRT is observed, either in the absence or presence of the three tested ligands. Taken together, these data reveal that LCA can selectively recruit RXR to liganded VDR, but does not promote interaction of VDR with any of the tested p160 coactivators or corepressor proteins.

In Vitro Binding of RXR and Comodulators to VDR Displays a Different Profile for $1,25(OH)_2D_3$-VDR Versus LCA- and 3-KetoLCA-VDR

In order to probe further the association of ligand-bound VDR and various comodulator proteins, including RXR and SRC-1, we employed GST based protein-protein "pulldown" assays. A GST-VDR fusion protein bound to Sepharose beads was used to test for interaction with in vitro transcribed/translated, [^{35}S]-labeled coregulators. Figure 7A shows that RXRα binds weakly to GST-VDR in the absence of ligand (lane 1), whereas GST control beads reveal no signal (data not shown). Importantly, RXRα-VDR dimerization is dramatically enhanced by $1,25(OH)_2D_3$, and to a lesser extent by LCA and the 3-keto-lithocholic acid metabolite (3-keto) (lanes 2–4). The inclusion of the CYP3A4 XDR3 VDRE in the binding reaction facilitates formation of the RXR–VDR complex even in the absence of any VDR ligand (lane 5), suggesting that the VDRE can serve as a scaffold to bring together the RXR and VDR proteins, essentially acting as a "pseudo" ligand. Further enhancement of RXR-VDR heterodimerization is observed with $1,25(OH)_2D_3$, LCA or 3-keto treatment (lanes 6–8). These data suggest that LCA- and 3-keto-VDR are less able to bind RXR than is $1,25(OH)_2D_3$-VDR, and the capacity of all liganded VDRs, especially LCA and 3-keto liganded VDR, to bind RXR is considerably enhanced in the presence of the DNA responsive element. A similar experiment was carried out utilizing both full-length human RXRα and SRC-1 (Fig. 7B). The results demonstrate that RXR association with VDR is substantially augmented in the presence of $1,25(OH)_2D_3$ but only modestly with LCA (lanes 4–5), while cholic acid does not generate a heterodimeric complex above that observed in the absence of ligand (compare lanes 3 and 6). A qualitatively analogous pattern of recruitment is observed when SRC-1 is incubated with GST-VDR and the various ligands (lanes 7–10). Co-incubation of RXR and SRC-1 along with the CYP3A4 XDR3 VDRE does not promote further enhancement of SRC-1 binding to VDR with any ligand tested, but does increase the interaction of RXR-VDR especially in the presence of LCA (compare lanes 5 and 13), thus reinforcing the results obtained in Figure 7A and implying that the affinity of LCA-VDR for either SRC-1 or RXR, even when boosted by the presence of a VDRE, is attenuated compared to that of $1,25(OH)_2D_3$-VDR.

Additional VDR comodulators tested by pull-down assay with GST-VDR included DRIP205, a key subunit of the mediator complex that interacts directly with nuclear receptors, as well as VDR, in a ligand dependent-manner, and anchors the other DRIP subunits to form the mediator complex [Rachez and Freedman, 2001]. Full-length DRIP205 binds to $1,25(OH)_2D_3$-VDR and to a lesser extent to LCA-VDR, but not to unliganded VDR (Fig. 7C, upper panel). The two other proteins evaluated in this system were NCoA-62, a VDR comodulator that appears to participate in spliceosome-mediated heterogeneous nuclear RNA processing [Zhang et al., 2003], and TRIP1 (the mammalian counterpart to yeast SUG1), a documented VDR-interacting protein [Masuyama and MacDonald, 1998] that stimulates VDR proteolysis in a process blocked by the 26S proteasome inhibitor, MG-132. In contrast to the results with DRIP205, interaction between VDR and NCoA-62 or TRIP1/SUG1, which is readily seen in the presence of $1,25(OH)_2D_3$, was not observed with LCA-VDR (Fig. 7C, lower panel). Finally, the ability of liganded VDR to associate with full-length versus a fragment (595–782) of SRC-1 that contains three LXXLL nuclear receptor interaction domains was assessed in the in vitro pulldown assay. As shown in Figure 7D, the potency of

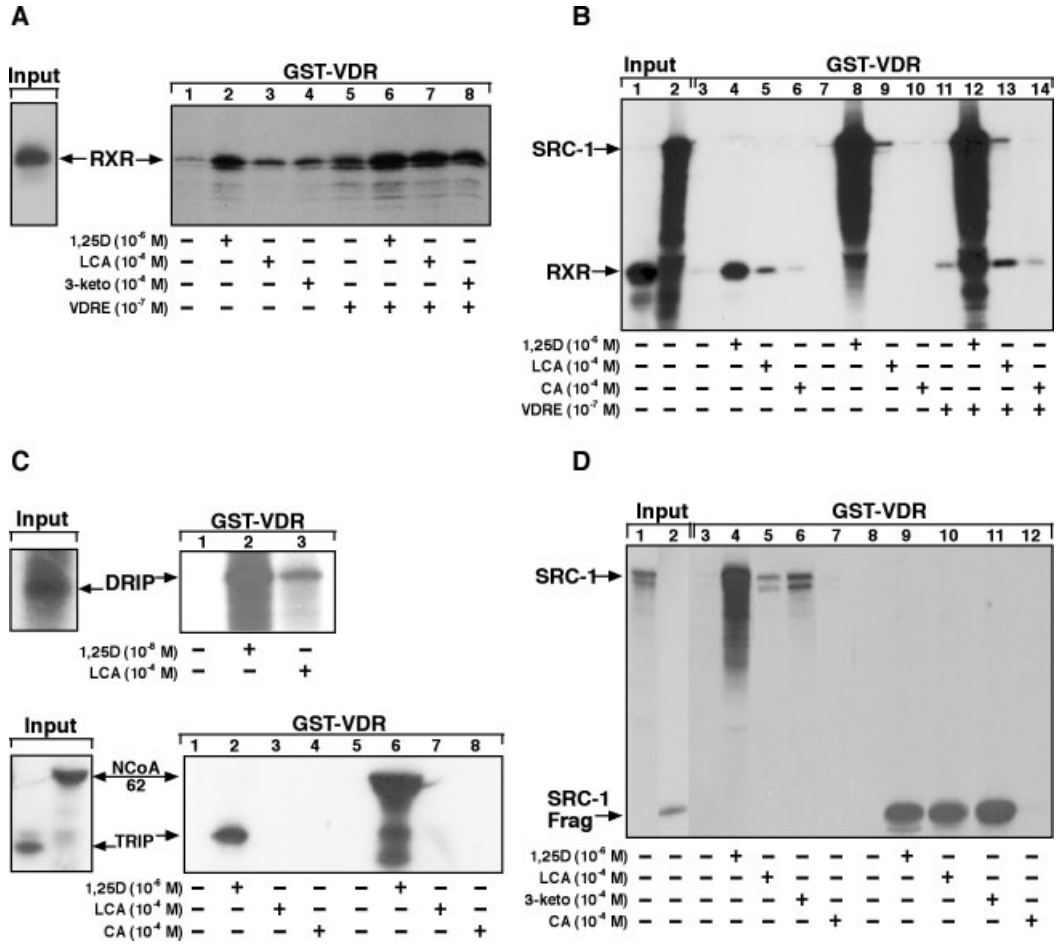

Fig. 7. Protein–protein interactions by LCA-VDR are distinct from those of $1,25(OH)_2D_3$-VDR. A GST-VDR fusion protein was used to assess binding of radiolabeled RXR or comodulators using a pulldown system. Aliquots (5%) of all radiolabeled protein inputs are shown in the far **left lanes** of each panel. **A**: Interaction with radiolabeled human RXRα in the presence of various ligands. 3-keto is 3-ketolithocholic acid. VDRE is a double-stranded oligonucleotide corresponding to the human CYP3A4 XDR3 VDRE. **B**: Interaction with RXR (**lanes 3–6**), SRC-1 (**lanes 7–10**), or both (**lanes 11–14**). The bile acid cholic acid (CA) does not bind VDR and serves as a negative control. **C**: Association of VDR with full-length human comodulators DRIP205 (DRIP), TRIP1, and NCoA-62. **D**: Interaction of VDR with full-length SRC-1 (**lanes 3–6**) versus a fragment of human SRC-1 (residues 595–782; **lanes 7–12**) containing three LXXLL domains.

ligand-stimulated binding to full-length SRC-1 is $1,25(OH)_2D_3 > 3\text{-keto} > LCA \gg CA$ (lanes 4–7). In sharp contrast, the 595–782 fragment of SRC-1 binds avidly to LCA-, 3-keto- and 1,25-VDRs and does not accurately reflect the relative affinities of these liganded VDRs for full-length SRC-1 in this setting (lanes 9–11). The results in Figure 7, taken together, argue that despite the fact that LCA is a bona fide ligand for VDR, it appears to induce a conformation of the VDR LBD that is sub-optimal for RXR and coactivator interactions. However, the presence of the VDRE, or truncation of the SRC-1 coactivator, seems to promote more favorable binding to these proteins by both LCA- and 3-keto-VDR.

Overexpression of RXR, SRC-1 and Other Comodulators Differentially Boosts the Activity of $1,25(OH)_2D_3$-VDR Versus LCA-VDR

To investigate further the role of several VDR coregulators in $1,25(OH)_2D_3$ and LCA-driven transcription, the effects of exogenous RXR, SRC-1, DRIP205, NCoA-62, and TRIP1/SUG1 on CYP3A4 VDRE-mediated transactivation were evaluated in transfection assays, utilizing the COS-7 cell line (Fig. 8A). In these cells that contain modest concentrations of endogenous RXR, the addition of the RXRα partner caused a mild amplification of the $1,25(OH)_2D_3$ transcriptional response, and an even more significant boost in LCA-mediated transactivation as

compared to the empty vector control that contains the same amount of SV40 promoter-driven pSG5 expression vector without the comodulator insert. A similar augmentation in $1,25(OH)_2D_3$ activity was apparent when an equal amount of SRC-1 was overexpressed. SRC-1 supplementation also resulted in an even more dramatic enhancement of LCA-VDR transcription. The increase in VDR-based activation was not significantly elevated with DRIP205 expression, and NCoA-62 also did not appear to affect VDR-driven transcription of the GH reporter gene, perhaps because the levels of these two proteins are more abundant in COS-7 cells. The results in Figure 8A illustrate that $1,25(OH)_2D_3$-bound VDR shows near maximal activity with the endogenous levels of RXR and coactivators present in COS-7 cells. In contrast, LCA-bound VDR displays only partial activity unless exogenous RXR or, especially, SRC-1 is supplied. In contrast to the results with RXR and SRC-1, it was observed that VDR-mediated transcriptional activation by $1,25(OH)_2D_3$ and LCA was suppressed by approximately 25% upon cotransfection of TRIP1/SUG1. TRIP1/SUG1 attenuation of VDR action was statistically significant, but not complete, possibly because TRIP1/SUG1 may require for its action the multiple ubiquitination of its target transcription factor, in this case VDR [Masuyama and MacDonald, 1998].

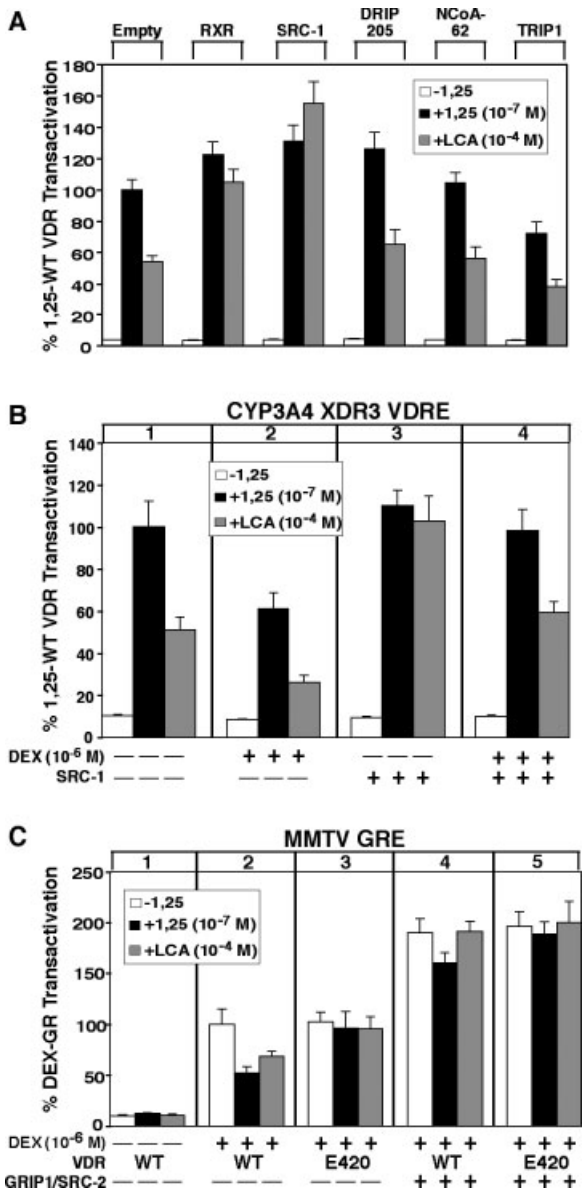

$1,25(OH)_2D_3$-VDR Is Superior to LCA-VDR in a GR Transcriptional Interference Assay

We next tested the ability of liganded VDR to participate in "coactivator crosstalk" by employing a transcriptional interference assay that included co-expression of VDR and GR in COS-7 cells. Figure 8B depicts the results in which COS-7 cells are cotransfected with the CYP3A4 VDRE-linked GH reporter gene and expression vectors for VDR and GR. Under these conditions, treatment with $1,25(OH)_2D_3$ or LCA results in a 10- and 5-fold increase, respectively, in the transcription of the GH reporter gene (panel 1). When the synthetic glucocorticoid, dexamethasone (DEX), is simultaneously added

Fig. 8. LCA-VDR has different affinities for RXR and coactivators relative to $1,25(OH)_2D_3$-VDR. **A**: Effect of exogenous RXR or comodulators on $1,25(OH)_2D_3$- (1,25) versus LCA-mediated transcription. COS-7 cells were cotransfected with a VDR vector along with a GH reporter construct containing the CYP3A4 XDR3 VDRE. Individual groups also received an expression plasmid for the indicated comodulator, RXR, or empty vector. TRIP1 is the mammalian counterpart to yeast SUG1. Secreted GH levels were normalized to the level with VDR in the presence of $1,25(OH)_2D_3$. **B**: Differential squelching by activated GR of $1,25(OH)_2D_3$ versus LCA function. COS-7 cells were transfected as in **panel A** plus an expression plasmid for mouse GR. Additional treatments included dexamethasone (DEX) and an expression plasmid for SRC-1, as indicated at bottom of panel. **C**: Differential ability of $1,25(OH)_2D_3$- versus LCA-bound VDR to squelch GR-mediated transactivation. COS-7 cells were transfected with a GR vector and a reporter construct containing the mouse mammary tumor virus glucocorticoid responsive element (MMTV GRE). The GH levels in this experiment reflect GR, and not VDR signaling. In addition to ligand treatments shown in inset, individual groups also received DEX, an expression plasmid for either wild-type VDR (WT) or the E420A helix-12 mutant, and/or an expression plasmid for the mouse coactivator GRIP1/SRC-2.

to cells dosed with $1,25(OH)_2D_3$ or LCA, the level of VDR-ligand stimulation of GH is reduced by 40%, presumably because activation of GR by the DEX ligand results in competition between GR and VDR for a limiting pool of shared coactivator molecules (panel 2). That exogenous SRC-1 can reduce this competition is confirmed by the results in panel 4, in which transactivation by both $1,25(OH)_2D_3$- and LCA-bound VDR is restored (compare panels 1 and 4). Finally, in the absence of DEX, exogenous SRC-1 boosts activation by LCA, but not $1,25(OH)_2D_3$ (panel 3). These results, taken together, suggest that in the absence of GR-DEX-mediated squelching, endogenous levels of SRC-1 (or equivalent p160 coactivators) are sufficient for $1,25(OH)_2D_3$-bound VDR but not for LCA-VDR. This interpretation is consistent with the observations in Figures 5–7 that suggest LCA-VDR has a lower affinity for SRC-1.

When the reverse experiment is performed (Fig. 8C) in which the transfected GH reporter vector consists of the GRE derived from the mouse mammary tumor virus (MMTV GRE) along with co-expressed VDR and GR, only treatment with DEX yields significant GH expression (compare panels 1 and 2). Simultaneous exposure of the transfected COS-7 cells to $1,25(OH)_2D_3$ or LCA reduces GR-mediated transactivation (panel 2). Overexpression of the GR p160 coactivator, GRIP1/SRC-2, not only boosts DEX-dependent GR transactivation, but also partially and fully restores GRE-mediated transcription in the presence of $1,25(OH)_2D_3$ and LCA, respectively (panel 4). Importantly, when an AF-2 mutant hVDR (E420A) that is transcriptionally inactive was utilized, transcriptional interference was not observed under any conditions tested (panels 3 and 5). These results demonstrate that liganded VDR can functionally interact with at least one transcriptional coactivator that also functions in GR-mediated signaling (even though GRIP1/SRC-2 binding is not potent in the mammalian two-hybrid system; Figure 6B,D), and that this association is dependent upon both the $1,25(OH)_2D_3$ or LCA ligand and the integrity of the VDR AF-2 domain. Moreover, LCA-bound VDR is slightly less able to squelch GR transactivation than is $1,25(OH)_2D_3$-bound VDR (panels 2 and 4). The data in Figure 8 reinforce the conclusion that LCA-VDR appears to have a lower affinity for RXR, SRC-1, and for endogenous coactivators present in COS-7 cells that interact with VDR and GR (possibly GRIP1/SRC-2).

Mutational Analysis Shows That $1,25(OH)_2D_3$, LCA and 3-KetoLCA Apparently Contact Several Distinct Residues in the Ligand Binding Pocket of VDR

Finally, an analysis was conducted within the VDR LBD to pinpoint which amino acids are required for $1,25(OH)_2D_3$ and/or LCA binding, and for transactivation in the helix-3/12 coactivator platform domain [Rochel et al., 2000]. We first examined the X-ray crystallographic structure of $1,25(OH)_2D_3$-liganded VDR [Rochel et al., 2000] to identify ligand binding residues. We then compared the amino acid sequences of hVDR and hPXR with particular attention to those regions known to be involved in ligand binding by either VDR or PXR [Watkins et al., 2001]. Our rationale was that, since PXR can bind LCA but not $1,25(OH)_2D_3$ [Makishima et al., 2002], any amino acids that differ between PXR and VDR might distinguish binding of LCA from $1,25(OH)_2D_3$. Two prominent examples of amino acids differences in these two receptors are the helix-3 residues serine-225 and serine-237 in hVDR, which are phenylalanine and methionine, respectively, in the hPXR sequence. Accordingly, mutants S225F and S237M were created in hVDR by site-directed mutagenesis. Also, two natural mutants of hVDR that confer the HVDRR phenotype were tested, namely R274L and I314S [Whitfield et al., 1996]. All other mutants of known or suspected ligand binding residues were changed to alanine, with the exceptions of C288G, a previously-published ligand binding mutation [Nakajima et al., 1996], and amino acids in the helix-3 (I238D) and helix-12 (V421D) p160 coactivator docking region. COS-7 cells were transfected with the VDR mutant plasmid along with a GH reporter gene containing the CYP3A4 VDRE or a luciferase reporter driven by the human CYP24 natural promoter. COS-7 cells were used for transfection because they do not contain significant levels of endogenous VDR. Figure 9A reveals that LCA and $1,25(OH)_2D_3$ appear to utilize overlapping, but distinct sets of ligand contacts and supporting structures. Both ligands seem to have a strong requirement for aspartate-232 (D232), isoleucine-271 (I271), arginine-274 (R274), cysteine-288 (C288), histidine-397 (H397), and

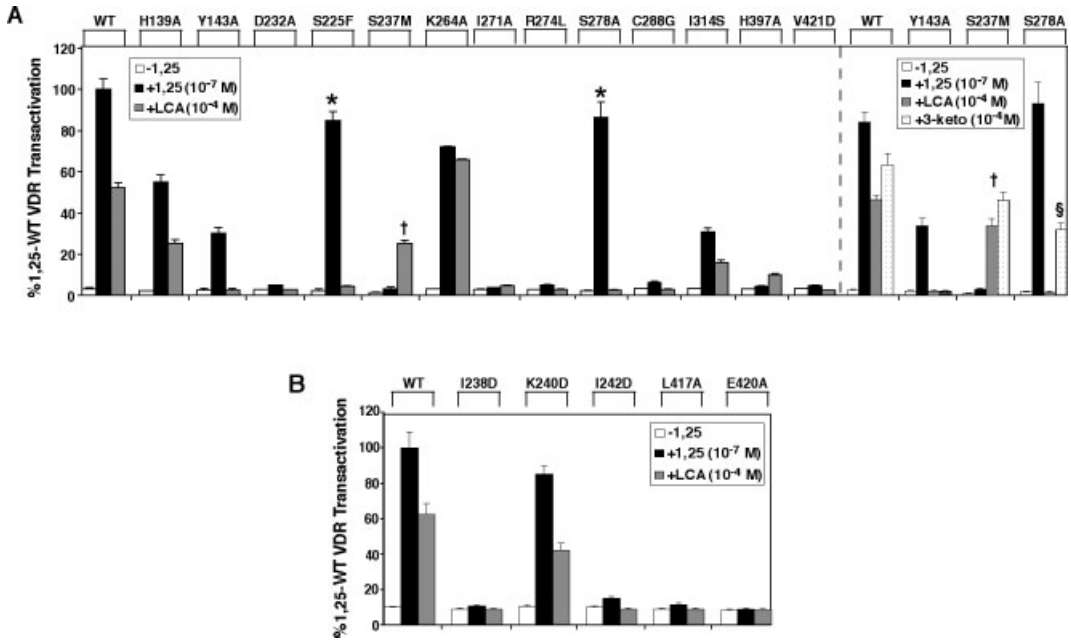

Fig. 9. Point mutants in hVDR distinguish contacts by different VDR ligands but not the coactivator binding platforms induced by those ligands. **A**: Transcriptional activation response of VDR point mutants to $1,25(OH)_2D_3$ (1,25) versus lithocholic acid (LCA). COS-7 cells were transfected with the indicated VDR mutant along with a GH reporter construct containing two copies of the XDR3 VDRE from the human *CYP3A4* gene, then incubated with $1,25(OH)_2D_3$, LCA, or ethanol vehicle (−1,25). Secreted GH levels were normalized to the level in the presence of wild-type VDR (WT) and $1,25(OH)_2D_3$. **Right panel** also shows the ability of 3-ketolithocholic acid (3-keto) to activate a subset of VDR mutants. This group of plates was transfected with a luciferase reporter construct containing the natural promoter from the human 24-hydroxylase gene. **B**: VDR point mutants in the helix-3 (I238D and I242D) or helix-12 (L417A and E420A) domains were tested for their ability to be activated by $1,25(OH)_2D_3$ or LCA as described for the left side of **panel A** using the GH reporter vector. The K240D VDR represents a helix-3 mutant that does not form part of the $1,25(OH)_2D_3$-induced coactivator platform.

valine-421 (V421). Mutation at histidine-139 (H139), tyrosine-143 (Y143), and isoleucine-314 (I314) also had a significant effect on activation by either ligand. In contrast, mutations of serine-225 (S225) or serine-278 (S278) affected only LCA-mediated transcription (indicated by *), whereas mutation of serine-237 (S237) abolished activation by $1,25(OH)_2D_3$ but not by LCA or its 3-keto derivative (indicated by †). The 3-ketolithocholic acid ligand also required tyrosine-143, but not serine-278 (S278), the latter observation (indicated by §) clearly distinguishing it from its LCA parent compound. A similar analysis (Fig. 9B) in COS-7 cells with helix-3 (I238D, K240D, and I242D) and helix-12 (L417A and E420A) VDR mutants illustrates that both $1,25(OH)_2D_3$ and LCA require the helix-3/12 coactivator platform, with the exception of lysine-240 (K240), a residue that does not participate in coactivator binding within this region [Vanhooke et al., 2004] and therefore serves as a negative control.

DISCUSSION

The results herein extend the original observation [Makishima et al., 2002], as well as two more recent studies [Choi et al., 2003; Adachi et al., 2004], of LCA as a functional VDR ligand. We show for the first time that LCA (as well as $1,25(OH)_2D_3$) is capable of inducing the endogenous *CYP3A4* gene and its protein product in HT-29 human colon cancer cells (Fig. 1), supplying direct evidence for the potential relevance of enhanced CYP3A4 expression in the recognized ability of vitamin D to reduce the incidence of high dietary fat associated colon cancer [Guyton et al., 2001]. Indeed, the participation of VDR in LCA detoxification is likely limited to the colon, a major locale for both high concentrations of LCA and elevated VDR expression [Berger et al., 1988]. Finally, because VDR null mice display hyperproliferation of colonic cells [Kallay et al., 2001], ligand-mediated activation of VDR appears to be crucial for normal cell growth and differentiation at this site.

The present study was also undertaken to determine if $1,25(OH)_2D_3$ and LCA confer ligand-specific conformations on liganded VDR that might be distinguishable in functional assays. The results (Figs. 6–8) argue that not only can VDRs bound to $1,25(OH)_2D_3$ or to LCA be clearly differentiated in their abilities to interact with RXR, full-length SRC-1, DRIP205, NCoA-62, and TRIP-1, but also that the 3-keto metabolite of LCA very likely confers yet a third conformational variation to VDR. In gel mobility shift, mammalian two-hybrid, VDR pulldown, VDR transcriptional activation, and transcription interference assays, a comparison of the results obtained with $1,25(OH)_2D_3$ versus LCA showed substantial differences, with the $1,25(OH)_2D_3$ ligand usually demonstrating superior activity. Interestingly, however, certain cell lines and VDREs seemed to support a maximum level of LCA-mediated transcription, which approached that mediated by $1,25(OH)_2D_3$, taking into account that the LCA ligand is approximately three orders of magnitude less potent on a molar basis. For instance, the HT-29 cell line transfected with either human CYP3A4 or rat CYP24 XDR3 VDRE reporter constructs yielded values of GH reporter expression by LCA-bound VDR that were nearly equal to those elicited by $1,25(OH)_2D_3$-bound VDR (Fig. 3B). Also, by supplying exogenous RXR or SRC-1 via transfection, transactivation by LCA-VDR in COS-7 cells could be boosted to nearly match levels of $1,25(OH)_2D_3$-mediated transactivation (Fig. 8A). On the other hand, certain cell lines and different VDREs appeared to accentuate the differences between the potency of LCA versus $1,25(OH)_2D_3$. For example, in ROS 17/2.8 bone cells transfected with a rat osteocalcin natural promoter VDRE-reporter construct, LCA was virtually transcriptionally inactive as a VDR ligand, even at a 10^{-4} M concentration, unless exogenous RXR was supplied (Fig. 4D, compare the third and seventh treatment groups). The simplest interpretation is that the LCA ligand is colon specific and does not encounter bone cells in vivo. However, another plausible explanation of these results is that LCA, as a lower affinity ligand, is apparently less efficacious than $1,25(OH)_2D_3$ in stabilizing a transcriptionally active conformation of VDR, but this deficit can be overcome in part by higher expression, in cells like those in the colon, of RXR and comodulators that participate in downstream VDR signaling. Moreover, the presumed allosteric influence on VDR of the RXR coreceptor [Thompson et al., 1998] and/or VDRE platforms with different sequences [Staal et al., 1996] could contribute to the efficacy of LCA as a VDR activating ligand.

Indeed, a "phantom ligand" network of residues in nuclear receptors recently has been identified [Shulman et al., 2004] that confers non-permissive receptors like VDR, which function as RXR heterodimers, with the ability to allosterically communicate with the RXR heteropartner. Mutation of the "phantom ligand" residues in VDR abolished LCA activity, but $1,25(OH)_2D_3$ stimulation of transcription was unaffected [Shulman et al., 2004], indicating that the lower affinity LCA ligand requires both the phantom ligand residues in VDR and cooperation with RXR to effect transactivation. This concept is in complete agreement with the current observation that LCA-VDR requires excess RXR for full activity, and suggests that RXR heterodimerization and perhaps additional multimerization with factors like SRC-1, are blunted when VDR is liganded with LCA instead of $1,25(OH)_2D_3$. Thus, in its more ancient role as a low affinity bile acid sensor, VDR depends on its "phantom ligand" allosteric network and bidirectional communication with RXR to activate transcription, whereas this allosteric network appears to be silent in the more evolutionarily advanced and high affinity endocrine response to $1,25(OH)_2D_3$.

Many of the current results can also be related to X-ray crystallographic studies of VDR [Rochel et al., 2000; Tocchini-Valentini et al., 2001, 2004; Vanhooke et al., 2004], and inferences can be made from the structure of FXR liganded to a semi-synthetic bile acid [Mi et al., 2003]. The VDR LBD from both human and rat has been crystallized, occupied by $1,25(OH)_2D_3$ and several vitamin D analogs, with the caveat that a 51-residue portion was removed from the hVDR LBD (residues 165–215), and a similar 46-residue portion (residues 165–211) was removed from the rat VDR LBD, in order to facilitate crystallization. In each of these X-ray structures, the VDR LBD consists of a canonical 12-helical triple sandwich with a hydrophobic, ligand-binding pocket. The rat VDR crystal structure ([Vanhooke et al., 2004]; protein database designation 1RK3) also contains, in addition to the $1,25(OH)_2D_3$ ligand, a 13-residue oligopeptide corresponding to the LXXLL

domain in the human DRIP205 coactivator [Rachez et al., 2000]. Crystallographic analyses of VDR bound to LCA or to 3-ketoLCA have not yet been reported, however, a modeling study is discussed by Choi et al. [2003], in which a few key ligand contacts are proposed.

Based upon the functional consequences of point mutation of key hVDR residues that line the hydrophobic pocket (Fig. 9), one set of specific distinctions that emerges between $1,25(OH)_2D_3$ and LCA as VDR ligands concerns the LBD residues that apparently contact these two different ligands (Fig. 9 and [Adachi et al., 2004]). This is not surprising, given the chemical differences between $1,25(OH)_2D_3$ and LCA as cholesterol-derived lipids. Thus, as illustrated schematically in Figure 10A–C, the observed apparent lack of interaction between LCA (or 3-ketoLCA) and the S237 residue in hVDR (Fig. 9) can be explained by an absence of a 1α-hydroxyl group in the A-ring of the two bile acid ligands. This 1α(OH)-S237 interaction is a

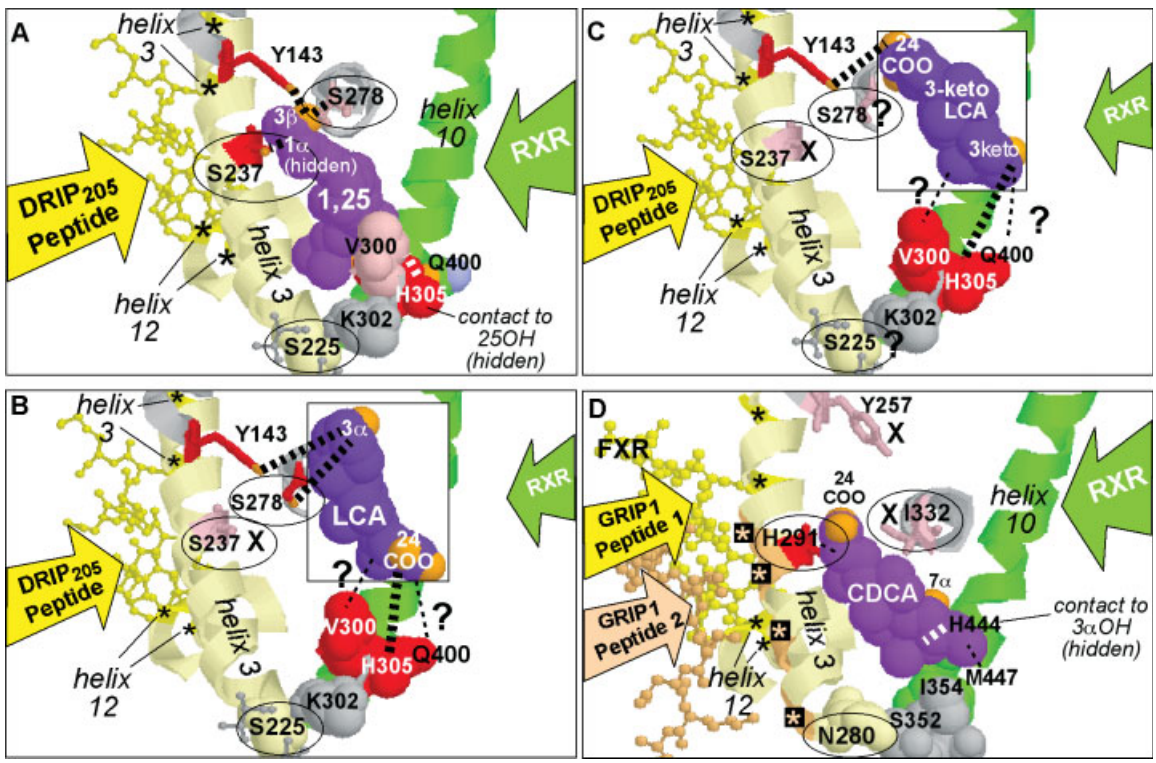

Fig. 10. Unique roles of serine-237 (S237), serine-278 (S278), and serine-225 (S225) in VDR bound to $1,25(OH)_2D_3$ (**Panel A**), LCA (**Panel B**), or 3-ketoLCA (**Panel C**). These three residues are circled, and the numbering used corresponds to hVDR (rat VDR numbering for these three residues is S221, S234, and S274). Residues that are proven or proposed ligand contacts are shown in red. **Panel D** is a view of rat FXR bound to 6α-ethylchenodeoxycholic acid (6ECDCA), a compound similar to LCA, and to two GRIP1 peptides. Residues that correspond to S225, S237, and S278 are circled. The views in panels A–C were created in Protein Explorer [Martz, 2002] from the coordinates of rat VDR bound to its $1,25(OH)_2D_3$ ligand and to an LXXLL peptide (protein database file 1RK3, described in [Vanhooke et al., 2004]). Interactions between VDR residues and either the LCA ligand (panel B) or the 3-ketoLCA ligand (panel C) are based on the modeling studies of Choi et al. [2003]. Panel D was created in Protein Explorer using the coordinates from file 1OSV, referenced in [Mi et al., 2003]. Representations of the LCA and 3-ketoLCA ligands were created by taking the crystal coordinates for chenodeoxycholic acid from file 1OSK (described in [Downes et al., 2003]) and hiding the 7α-hydroxyl moiety. Hydrogen bonds between receptor LBD residues and ligand are indicated by a heavy dotted line. Van der Waals interactions are denoted by a finer dotted line. An X indicates the lack of a hydrogen bond that occurs in a least one other structure. Question marks in panels B and C suggest likely interactions between VDR and either LCA or 3-ketoLCA that were not found (or not mentioned) in the modeling studies by Choi et al. [2003]. The yellow arrows at the left of each panel represent coactivators that have been shown to interact with helices-3 and -12 (shown in light yellow); a smaller arrow in panels B and C indicates an attenuated interaction relative to that of $1,25(OH)_2D_3$-bound VDR. Actual coactivator peptides are shown in yellow in ball-and-stick format (the second LXXLL peptide in panel D is depicted in light orange). Residues in either VDR or FXR that contact coactivator peptides are denoted by asterisks. The green arrows at the right of each panel indicate the RXR dimer partner that interacts with helix-10 (shown in green); the smaller size of the arrow in panels B and C refers to the observed attenuation of this interaction in LCA- and 3-ketoLCA-bound VDRs.

prominent feature of $1,25(OH)_2D_3$-bound VDR [Rochel et al., 2000], in which a hydrogen bond is formed between the 1α-OH of the ligand and the hydroxyl group of the S237 side chain. The lack of this hydrogen bond likely accounts, at least in part, for the fact that the affinity of both LCA and 3-ketoLCA for VDR is greatly reduced compared to that of $1,25(OH)_2D_3$ [Makishima et al., 2002]. In addition, the 1α(OH)-S237 interaction may be important for configuring helix-3 in $1,25(OH)_2D_3$-bound VDR for optimal interaction with coactivators containing LXXLL motifs (Fig. 10A). Therefore, in LCA-bound VDR, the absence of the 1α(OH)-S237 contact may contribute to suboptimal interactions of helix-3 with coactivators such as SRC-1 (Fig. 10, panels B and C; Fig. 11A). 3-ketoLCA also lacks a 1α-hydroxyl group, but an additional consideration is that the 3-ketoLCA ligand is thought to enter the VDR ligand-binding pocket in an orientation that is reversed relative to either $1,25(OH)_2D_3$ or LCA ([Choi et al., 2003]; see discussion below). As shown in Figure 9A, S237M VDR activates transcription strongly in the presence of 3-ketoLCA, intimating that S237 is largely irrelevant for binding this LCA metabolite. In contrast, mutation of tyrosine-143 (Y143) markedly reduces transactivation by both $1,25(OH)_2D_3$- and bile acid-occupied VDRs (Fig. 9). Y143 forms a hydrogen bond to the 3β-hydroxyl group of $1,25(OH)_2D_3$ and also van der Waals contacts to the A-ring of the $1,25(OH)_2D_3$ ligand in both human and rat VDRs ([Rochel et al., 2000; Vanhooke et al., 2004]; see also Figs. 10A and 11B). Since an intact A-ring and a 3-hydroxyl moiety are also found in LCA, this interaction likely plays a similar role in LCA-bound VDR, even though the 3-hydroxyl group in LCA is in the α-configuration (Figs. 10B and 11A). Moreover, we speculate that Y143 might contact one of the oxygens in the 3-ketoLCA 24-carboxylic acid group (24COO) (Fig. 10C), a possible explanation for the strong negative effect of the Y143A mutation on transactivation by this ligand described herein (Fig. 9A) and by other groups [Choi et al., 2003; Adachi et al., 2004].

Mutation of a second residue in helix-3, namely serine-225 (S225), also exerts differential effects on transactivation by $1,25(OH)_2D_3$-bound versus LCA-bound VDR. In this case, however, it is LCA-mediated transcription that proves to be more sensitive. A structural explanation for this is suggested in Figure 10B. S225 is not a direct ligand contact, at least for $1,25(OH)_2D_3$, but instead exists as part of a chain of contacts that culminates in residues that have roles in both ligand interaction and dimerization. S225, at the N-terminal end of helix-3, is hemmed in by valines 157 and 159 (shown in ball-and-stick format in Fig. 10, panels A, B, and C), such that the S225 side chain faces toward lysine-302 (K302) in helix-6 of VDR. K302, for its part, contacts valine-300 (V300), and V300 touches histidine-305 (H305; both V300 and H305 are also in helix-6). H305 then contacts glutamine-400 (Q400), a residue in helix-10. One clue to the differential significance of the S225 residue for $1,25(OH)_2D_3$-bound versus LCA-bound VDR is suggested by the mutagenesis results of Choi et al. [2003], who determined that mutation of V300, H305, and Q400 (each to alanine) all had a greater effect on LCA-mediated transcription than on $1,25(OH)_2D_3$-mediated transcription. The results with V300A, H305A, and Q400A have been confirmed in other published studies [Choi et al., 2001; Adachi et al., 2004]. The present mutation of S225 to phenylalanine, which has not been previously reported, places a much larger residue at position 225, which might be expected to displace the entire S225–K302–V300–H305–Q400 series of interactions. This displacement would likely to have a much more serious cumulative impact on transactivation by LCA than by $1,25(OH)_2D_3$, since these residues appear to play a more important role in LCA-mediated transactivation. An important point concerns the location of Q400. This residue, positioned at the terminus of this series of interactions, resides in helix-10, which forms part of the dimer interface (see. Fig. 11B). The fact that V300 and H305, the two residues that precede Q400 in the chain of interactions, have a very different significance for LCA-bound VDR than for $1,25(OH)_2D_3$-bound VDR, plus the observation that LCA-bound VDR displays significantly less affinity for RXR than does $1,25(OH)_2D_3$-bound VDR (Figs. 6 and 7), suggests that the series of V300–H305–Q400 interactions contribute to a different, and less optimal, helix-10 configuration when LCA is bound to VDR (Figs. 10B and 11A). Thus, we propose that the positioning of helix-10 is suboptimal in bile acid-occupied VDR, resulting in attenuated RXR attraction for VDRE binding and coactivator recruitment (Figs. 10B,C and 11A vs. Figs. 10A and 11B).

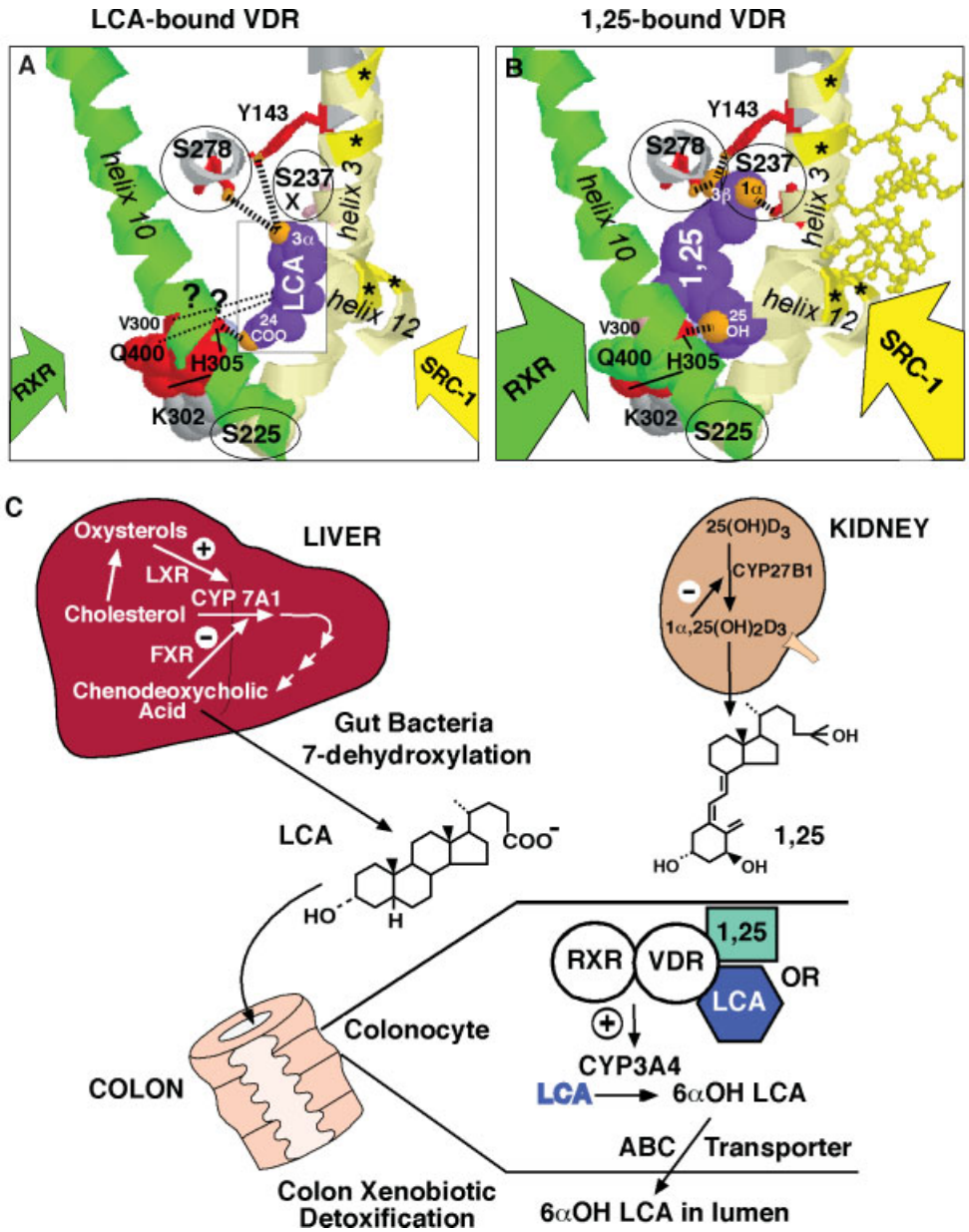

Fig. 11. Differential binding of $1,25(OH)_2D_3$ and LCA to VDR and an integrative model for the physiologic significance in humans of LCA as a VDR ligand. View of the VDR LBD from the opposite side to that seen in Figure 10. **A**: LCA-bound VDR LBD and its attenuated interactions with RXR and SRC-1, as indicated by smaller arrows than with $1,25(OH)_2D_3$-VDR in (B). Hydrogen bonds and van der Waals interactions are depicted by dotted heavy or light lines, respectively. The LCA ligand is shown in reduced size for clarity. The three residues for which mutation yields differential effects with $1,25(OH)_2D_3$- versus LCA-bound VDR are circled. As described in Figure 10, interactions between the LCA ligand and hVDR residues are based on the modeling of Choi et al. [2003]. **B**: A view of the rat VDR LBD (with hVDR numbering) bound to $1,25(OH)_2D_3$ and also to a 13-residue SRC-1 peptide [Vanhooke et al., 2004]. **C**: Physiologic roles of two VDR ligands. LCA (left side) is produced from liver-derived chenodeoxycholic acid (also abbreviated CDCA) by the action of gut bacteria. LCA, which is not recycled in the terminal ileum due to the loss of the 7α-hydroxyl, instead travels to the colon, where it can exert tumorigenic actions on the colonocyte (see text). However, the ability of VDR to bind LCA and activate the *CYP3A4* gene may allow for detoxification of LCA by 6α-hydroxylation and export via the ABC efflux transporter.

A final VDR residue for which mutation shows a differential effect on $1,25(OH)_2D_3$- versus LCA-mediated transactivation is serine-278 (S278). In this case, only transactivation by LCA was seriously compromised (Fig. 9A, last set of bars); transactivation by $1,25(OH)_2D_3$ or 3-ketoLCA remained relatively unaffected. Apparently, the hydrogen bond between S278 and

the 3β-OH on $1,25(OH)_2D_3$ is of minor significance compared to that involving the 3α-OH of LCA, perhaps because $1,25(OH)_2D_3$ possesses the strong 1α(OH)-S237 bond nearby, as well as an interaction with Y143 for yet a second "back-up" hydrogen bond in the vicinity (Fig. 10A). Further, mutation of S278 to alanine (S278A) is able to distinguish LCA-bound VDR from 3-ketoLCA-bound VDR. Paradoxically, in the modeling study of Choi et al. [2003], one of the oxygens in the 24COO of 3-ketoLCA is within hydrogen bond distance to S278 (recall that 3-ketoLCA enters the binding pocket inverted relative to either $1,25(OH)_2D_3$ or LCA, such that the side chain oxygens are close to S278, rather than being near H305 as they would be for LCA; compare Fig. 10, panels B and C). However, as introduced above, we speculate that the other oxygen in the 24COO of 3-ketoLCA might be interacting with the hydroxyl group of tyrosine-143 (Y143; Fig. 10C), since a Y143A mutation nearly abolishes transactivation by 3-ketoLCA (Fig. 9A). Taking this speculation one step further, it is possible that the 24-carboxyl-Y143 interaction can anchor the 3-ketoLCA ligand even in the absence of the S278 hydroxyl group, providing a "back-up" hydrogen bond for 3-ketoLCA analogous to the 1α(OH)-S237 bond that overcomes the loss of S278 with respect to $1,25(OH)_2D_3$ action.

As mentioned above, the position of the 3-ketoLCA ligand in the VDR LBD, as presented in Figure 10C, is reversed relative to the positions of either $1,25(OH)_2D_3$ or LCA; thus, the side chain of 3-ketoLCA with its 24COO faces toward Y143 and S278, rather than being oriented toward H305 as with LCA (compare Fig. 10B and C). This configuration of 3-ketoLCA is based primarily on the modeling study of Choi et al. [2003]. Additional evidence that such a configuration is possible with a bile acid ligand is provided by another crystallographic study with a related receptor, human FXR [Mi et al. 2003]. As shown in Figure 10D, the FXR LBD has been crystallized with 6α-ethylchenodeoxycholic acid (6ECDCA). 6ECDCD is a bile acid that is closely related to LCA, differing only in having a synthetic 6α-ethyl group and a 7α-hydroxyl (as explained above and in Fig. 11C, the 7α-hydroxyl, placed on all natural bile acids during their synthesis in the liver, is removed from CDCA by the action of intestinal bacteria to produce LCA, which can then be modified to 3-ketoLCA). In the FXR LBD-6ECDCA crystal (Fig. 10D), the position of the bile acid ligand is very similar to the modeling of 3-ketoLCA in the VDR LBD. The similarity is especially strong with respect to the 3-keto group of 3-ketoLCA and the 3α-hydroxyl of 6ECDCA. In each case, the oxygen atom attached to the 3-carbon forms a hydrogen bond to a histidine residue that is positionally conserved in both receptors (H305 in hVDR and H444 in hFXR). The position of the side chain is, however, somewhat different: in the Choi model, the 24COO group forms a hydrogen bond with S278 in hVDR, whereas in the FXR LBD-6ECDCA structure, this same hydrogen bond cannot occur since the residue in FXR corresponding to S278 is an isoleucine (I332). Instead, the 24COO of FXR bends over toward helix-3, where it establishes van der Waals contacts with histidine-291 (H291, the positional equivalent of S237 in hVDR) [Mi et al., 2003].

In summary, as depicted in Figure 11A,B, LCA and $1,25(OH)_2D_3$ apparently lie in similar orientations in the VDR ligand binding pocket, both employing hydrogen bonding with hVDR residues Y143/S278 for the A-ring hydroxyl group and with H305 for the side chain OH/COOH functional groups. Whereas both of these VDR ligands require Y143 and H305 for receptor binding/activation, the key differences supporting VDR ligand contact and receptor activation are that LCA absolutely requires S278 and a small side chain at position 225, while $1,25(OH)_2D_3$ depends instead on hydrogen bonding of its unique 1α-OH group to S237. As depicted by smaller arrows in Figure 11A versus 11B, we conclude that LCA binding suboptimally conforms VDR in two fashions: (i) a less ideal positioning of helix-10 to create the RXR interface, and (ii) a somewhat destabilized helix-3/helix-12 platform for docking of p160 coactivators like SRC-1. Therefore, the results of mutation of crucial VDR residues that contribute differentially to LCA versus $1,25(OH)_2D_3$ activation of VDR allows one to deduce the potential mechanisms to explain the observations that LCA, while a definitive stimulator of VDR-mediated transactivation, is unable to conform the RXR coreceptor and coactivator surfaces of the receptor optimally. In fact, LCA could generate unique VDR conformations that recruit different comodulators than $1,25(OH)_2D_3$-VDR, or, alternatively, LCA-bound VDR might recognize distinct

VDRE platforms in the promoter region of genes specifically or preferentially regulated by this ligand. The ultimate structural test of this hypothesis must await the crystallization and X-ray diffraction analysis of VDR occupied by its low affinity bile acid ligands.

Finally, a hypothetical model for the pathophysiologic significance in humans of LCA as a VDR ligand is depicted in Figure 11C. The precursor to LCA, CDCA, is produced in the liver via a pathway that is controlled in a positive fashion by LXR and in a negative feedback loop by FXR [Chawla et al., 2001; Lu et al., 2001] (both of these receptors form heterodimers with RXR, not shown). LCA, formed through 7-dehydroxylation by gut bacteria, is not a good substrate for the enterohepatic bile acid reuptake system, and thus remains in the enteric tract and passes to the colon, where it can exert carcinogenic effects [Kozoni et al., 2000]. VDR in the colonocyte is proposed to bind LCA or its 3-keto derivative and activate CYP3A4 [Makishima et al., 2002]. CYP3A4 then catalyzes the 6α-hydroxylation of LCA [Araya and Wikvall, 1999], thus converting it into a substrate for the ABC efflux transporter [Chawla et al., 2001]. We (Fig. 1 and [Thompson et al., 2002]) and others [Thummel et al., 2001] have shown that $1,25(OH)_2D_3$, which is formed in the kidney via the action of CYP27B1, can also activate CYP3A4. Thus, natural ligands for VDR, including the high affinity $1,25(OH)_2D_3$ hormonal metabolite and the lower affinity, nutritionally-modulated bile acids, seem to possess the important potential to serve as agents for promoting detoxification of LCA and possibly other intestinal endo- or xenobiotics, with the end result likely being a reduction in colon cancer incidence. It is intriguing to consider that additional, naturally occurring VDR ligands with similar, or even complementary, activities may remain to be discovered.

ACKNOWLEDGMENTS

This work was supported in part by National Institutes of Health Grants DK33351 and DK063930 (to M.R.H). We thank Professor David J. Mangelsdorf, University of Texas Southwestern Medical Center, for consultations on LCA as a VDR ligand and for comments on the manuscript. The authors thank Michelle Thatcher for preparation of the figures.

REFERENCES

Adachi R, Shulman AI, Yamamoto K, Shimomura I, Yamada S, Mangelsdorf DJ, Makishima M. 2004. Structural determinants for vitamin D receptor response to endocrine and xenobiotic signals. Mol Endocrinol 18: 43–52.

Araya Z, Wikvall K. 1999. 6alpha-hydroxylation of taurochenodeoxycholic acid and lithocholic acid by CYP3A4 in human liver microsomes. Biochim Biophys Acta 1438: 47–54.

Baker AR, McDonnell DP, Hughes MR, Crisp TM, Mangelsdorf DJ, Haussler MR, Pike JW, Shine J, O'Malley BW. 1988. Cloning and expression of full-length cDNA encoding human vitamin D receptor. Proc Natl Acad Sci USA 85:3294–3298.

Baudino TA, Kraichely DM, Jefcoat SC, Jr., Winchester SK, Partridge NC, MacDonald PN. 1998. Isolation and characterization of a novel coactivator protein, NCoA-62, involved in vitamin D-mediated transcription. J Biol Chem 273:16434–16441.

Berger U, Wilson P, McClelland RA, Colston K, Haussler MR, Pike JW, Coombes RC. 1988. Immunocytochemical detection of 1,25-dihydroxyvitamin D receptors in normal human tissues. J Clin Endocrinol Metab 67:607–613.

Bourguet W, Ruff M, Chambon P, Gronemeyer H, Moras D. 1995. Crystal structure of the ligand-binding domain of the human nuclear receptor RXR-α. Nature 375:377–382.

Boyle WJ, Simonet WS, Lacey DL. 2003. Osteoclast differentiation and activation. Nature 423:337–342.

Chawla A, Repa JJ, Evans RM, Mangelsdorf DJ. 2001. Nuclear receptors and lipid physiology: Opening the X-files. Science 294:1866–1870.

Chen H, Lin RJ, Schiltz RL, Chakravarti D, Nash A, Nagy L, Privalsky ML, Nakatani Y, Evans RM. 1997. Nuclear receptor coactivator ACTR is a novel histone acetyltransferase and forms a multimeric activation complex with P/CAF and CBP/p300. Cell 90:569–580.

Choi M, Yamamoto K, Masuno H, Nakashima K, Taga T, Yamada S. 2001. Ligand recognition by the vitamin D receptor. Bioorg Med Chem 9:1721–1730.

Choi M, Yamamoto K, Itoh T, Makishima M, Mangelsdorf DJ, Moras D, DeLuca HF, Yamada S. 2003. Interaction between vitamin D receptor and vitamin D ligands. Two-dimensional alanine scanning mutational analysis. Chem Biol 10:261–270.

Christakos S, Dhawan P, Liu Y, Peng X, Porta A. 2003. New insights into the mechanisms of vitamin D action. J Cell Biochem 88:695–705.

Danielsen M, Hinck L, Ringold GM. 1989. Mutational analysis of the mouse glucocorticoid receptor. Cancer Res 49(8 Suppl):2286s–2291s.

Downes M, Verdecia MA, Roecker AJ, Hughes R, Hogenesch JB, Kast-Woelbern HR, Bowman ME, Ferrer JL, Anisfeld AM, Edwards PA, Rosenfeld JM, Alvarez JG, Noel JP, Nicolaou KC, Evans RM. 2003. A chemical, genetic, and structural analysis of the nuclear bile acid receptor FXR. Mol Cell 11:1079–1092.

Drocourt L, Ourlin JC, Pascussi JM, Maurel P, Vilarem MJ. 2002. Expression of CYP3A4, CYP2B6, and CYP2C9 is regulated by the vitamin D receptor pathway in primary human hepatocytes. J Biol Chem 277:25125–25132.

Gill RK, Atkins LM, Hollis BW, Bell NH. 1998. Mapping the domains of the interaction of the vitamin D receptor and steroid receptor coactivator-1. Mol Endocrinol 12:57–65.

Green S, Isseman I, Sheer E. 1988. A versatile in vivo and in vitro eukaryotic expression vector for protein engineering. Nucleic Acids Res 16:369.

Gutierrez S, Liu J, Javed A, Montecino M, Stein GS, Lian JB, Stein JL. 2004. The vitamin D response element in the distal osteocalcin promoter contributes to chromatin organization of the proximal regulatory domain. J Biol Chem 279:43581–43588.

Guyton KZ, Kensler TW, Posner GH. 2001. Cancer chemoprevention using natural vitamin D and synthetic analogs. Annu Rev Pharmacol Toxicol 41:421–442.

Hamada K, Umemoto A, Kajikawa A, Seraj MJ, Monden Y. 1994. In vitro formation of DNA adducts with bile acids. Carcinogenesis 15:1911–1915.

Haussler MR, Whitfield GK, Haussler CA, Hsieh J-C, Thompson PD, Selznick SH, Encinas Dominguez C, Jurutka PW. 1998. The nuclear vitamin D receptor: Biological and molecular regulatory properties revealed. J Bone Miner Res 13:325–349.

Hong H, Kohli K, Garabedian MJ, Stallcup MR. 1997. GRIP1, a transcriptional coactivator for the AF-2 transactivation domain of steroid, thyroid, retinoid, and vitamin D receptors. Mol Cell Biol 17:2735–2744.

Honkakoski P, Negishi M. 2000. Regulation of cytochrome P450 (*CYP*) genes by nuclear receptors. Biochem J 347: 321–337.

Hsieh J-C, Jurutka PW, Galligan MA, Terpening CM, Haussler CA, Samuels DS, Shimizu Y, Shimizu N, Haussler MR. 1991. Human vitamin D receptor is selectively phosphorylated by protein kinase C on serine 51, a residue crucial to its trans-activation function. Proc Natl Acad Sci USA 88:9315–9319.

Huss JM, Kasper CB. 2000. Two-stage glucocorticoid induction of CYP3A23 through both the glucocorticoid and pregnane X receptors. Mol Pharmacol 58:48–57.

Huss JM, Wang SI, Astrom A, McQuiddy P, Kasper CB. 1996. Dexamethasone responsiveness of a major glucocorticoid-inducible *CYP3A* gene is mediated by elements unrelated to a glucocorticoid receptor binding motif. Proc Natl Acad Sci USA 93:4666–4670.

Jin CH, Kerner SA, Hong MH, Pike JW. 1996. Transcriptional activation and dimerization functions in the human vitamin D receptor. Mol Endocrinol 10:945–957.

Jones G, Strugnell SA, DeLuca HF. 1998. Current understanding of the molecular actions of vitamin D. Physiol Rev 78:1193–1231.

Jurutka PW, Hsieh J-C, MacDonald PN, Terpening CM, Haussler CA, Haussler MR, Whitfield GK. 1993. Phosphorylation of serine 208 in the human vitamin D receptor: The predominant amino acid phosphorylated by casein kinase II, in vitro, and identification as a significant phosphorylation site in intact cells. J Biol Chem 268:6791–6799.

Jurutka PW, Remus LS, Whitfield GK, Galligan MA, Haussler CA, Haussler MR. 2000. Biochemical evidence for a 170-kilodalton, AF-2-dependent vitamin D receptor/retinoid X receptor coactivator that is highly expressed in osteoblasts. Biochem Biophys Res Commun 267:813–819.

Jurutka PW, Whitfield GK, Hsieh J-C, Thompson PD, Haussler CA, Haussler MR. 2001. Molecular nature of the vitamin D receptor and its role in regulation of gene expression. Rev Endocr Metab Disord 2:203–216.

Kallay E, Pietschmann P, Toyokuni S, Bajna E, Hahn P, Mazzucco K, Bieglmayer C, Kato S, Cross HS. 2001. Characterization of a vitamin D receptor knockout mouse as a model of colorectal hyperproliferation and DNA damage. Carcinogenesis 22:1429–1435.

Kawaura A, Tanida N, Sawada K, Oda M, Shimoyama T. 1989. Supplemental administration of 1 alpha-hydroxyvitamin D_3 inhibits promotion by intrarectal instillation of lithocholic acid in N-methyl-N-nitrosourea-induced colonic tumorigenesis in rats. Carcinogenesis 10:647–649.

Kitagawa H, Fujiki R, Yoshimura K, Mezaki Y, Uematsu Y, Matsui D, Ogawa S, Unno K, Okubo M, Tokita A, Nakagawa T, Ito T, Ishimi Y, Nagasawa H, Matsumoto T, Yanagisawa J, Kato S. 2003. The chromatin-remodeling complex WINAC targets a nuclear receptor to promoters and is impaired in Williams syndrome. Cell 113:905–917.

Kitazawa R, Kitazawa S. 2002. Vitamin D_3 augments osteoclastogenesis via vitamin D-responsive element of mouse RANKL gene promoter. Biochem Biophys Res Commun 290:650–655.

Kliewer SA. 2003. The nuclear pregnane X receptor regulates xenobiotic detoxification. J Nutr 133:2444S–2447S.

Kliewer SA, Umesono K, Mangelsdorf DJ, Evans RM. 1992. Retinoid X receptor interacts with nuclear receptors in retinoic acid, thyroid hormone and vitamin D_3 signalling. Nature 355:446–449.

Kliewer SA, Moore JT, Wade L, Staudinger JL, Watson MA, Jones SA, McKee DD, Oliver BB, Willson TM, Zetterstrom RH, Perlmann T, Lehmann JM. 1998. An orphan nuclear receptor activated by pregnanes defines a novel steroid signaling pathway. Cell 92:73–82.

Kozoni V, Tsioulias G, Shiff S, Rigas B. 2000. The effect of lithocholic acid on proliferation and apoptosis during the early stages of colon carcinogenesis: differential effect on apoptosis in the presence of a colon carcinogen. Carcinogenesis 21:999–1005.

Lee JW, Choi H-S, Gyuris J, Brent R, Moore DD. 1995. Two classes of proteins dependent on either the presence or absence of thyroid hormone for interaction with the thyroid hormone receptor. Mol Endocrinol 9:243–254.

Lehmann JM, McKee DD, Watson MA, Willson TM, Moore JT, Kliewer SA. 1998. The human orphan nuclear receptor PXR is activated by compounds that regulate CYP3A4 gene expression and cause drug interactions. J Clin Invest 102:1016–1023.

Li YC, Pirro AE, Amling M, Delling G, Baron R, Bronson R, Demay MB. 1997. Targeted ablation of the vitamin D receptor: An animal model of vitamin D-dependent rickets type II with alopecia. Proc Natl Acad Sci USA 94:9831–9835.

Lu TT, Repa JJ, Mangelsdorf DJ. 2001. Orphan nuclear receptors as eLiXiRs and FiXeRs of sterol metabolism. J Biol Chem 276:37735–37738.

Luo G, Cunningham M, Kim S, Burn T, Lin J, Sinz M, Hamilton G, Rizzo C, Jolley S, Gilbert D, Downey A, Mudra D, Graham R, Carroll K, Xie J, Madan A, Parkinson A, Christ D, Selling B, LeCluyse E, Gan LS. 2002. CYP3A4 induction by drugs: Correlation between a pregnane X receptor reporter gene assay and CYP3A4

expression in human hepatocytes. Drug Metab Dispos 30:795–804.

MacDonald PN, Dowd DR, Nakajima S, Galligan MA, Reeder MC, Haussler CA, Ozato K, Haussler MR. 1993. Retinoid X receptors stimulate and 9-*cis* retinoic acid inhibits 1,25-dihydroxyvitamin D_3-activated expression of the rat osteocalcin gene. Mol Cell Biol 13:5907–5917.

Makishima M, Lu TT, Xie W, Whitfield GK, Domoto H, Evans RM, Haussler MR, Mangelsdorf DJ. 2002. Vitamin D receptor as an intestinal bile acid sensor. Science 296:1313–1316.

Malloy PJ, Pike JW, Feldman D. 1999. The vitamin D receptor and the syndrome of hereditary 1,25-dihydroxyvitamin D-resistant rickets. Endocr Rev 20:156–188.

Mangelsdorf DJ, Ong ES, Dyck JA, Evans RM. 1990. Nuclear receptor that identifies a novel retinoic acid response pathway. Nature 345:224–229.

Markose ER, Stein JL, Stein GS, Lian JB. 1990. Vitamin D-mediated modifications in protein-DNA interactions at two promoter elements of the osteocalcin gene. Proc Natl Acad Sci USA 87:1701–1705.

Martz E. 2002. Protein explorer: Easy yet powerful macromolecular visualization. Trends Biochem Sci 27:107–109.

Masuyama H, MacDonald PN. 1998. Proteasome-mediated degradation of the vitamin D receptor (VDR) and a putative role for SUG1 interaction with the AF-2 domain of VDR. J Cell Biochem 71:429–440.

McKenna NJ, O'Malley BW. 2002. Minireview: Nuclear receptor coactivators-an update. Endocrinology 143: 2461–2465.

McKenna NJ, Lanz RB, O'Malley BW. 1999a. Nuclear receptor coregulators: Cellular and molecular biology. Endocr Rev 20:321–344.

McKenna NJ, Xu J, Nawaz Z, Tsai SY, Tsai MJ, O'Malley BW. 1999b. Nuclear receptor coactivators: Multiple enzymes, multiple complexes, multiple functions. J Steroid Biochem Mol Biol 69:3–12.

Mi LZ, Devarakonda S, Harp JM, Han Q, Pellicciari R, Willson TM, Khorasanizadeh S, Rastinejad F. 2003. Structural basis for bile acid binding and activation of the nuclear receptor FXR. Mol Cell 11:1093–1100.

Nagengast FM, Grubben MJ, van Munster IP. 1995. Role of bile acids in colorectal carcinogenesis. Eur J Cancer 31A:1067–1070.

Nakajima S, Hsieh J-C, MacDonald PN, Galligan MA, Haussler CA, Whitfield GK, Haussler MR. 1994. The C-terminal region of the vitamin D receptor is essential to form a complex with a receptor auxiliary factor required for high affinity binding to the vitamin D responsive element. Mol Endocrinol 8:159–172.

Nakajima S, Hsieh J-C, Jurutka PW, Galligan MA, Haussler CA, Whitfield GK, Haussler MR. 1996. Examination of the potential functional role of conserved cysteine residues in the hormone binding domain of the human 1,25-dihydroxyvitamin D_3 receptor. J Biol Chem 271:5143–5149.

Noda M, Vogel RL, Craig AM, Prahl J, DeLuca HF, Denhardt DT. 1990. Identification of a DNA sequence responsible for binding of the 1,25-dihydroxyvitamin D_3 receptor and 1,25-dihydroxyvitamin D_3 enhancement of mouse secreted phosphoprotein 1 (Spp-1 or osteopontin) gene expression. Proc Natl Acad Sci USA 87:9995–9999.

Ohyama Y, Ozono K, Uchida M, Shinki T, Kato S, Suda T, Yamamoto O, Noshiro M, Kato Y. 1994. Identification of a vitamin D-responsive element in the 5′ flanking region of the rat 25-hydroxyvitamin D_3 24-hydroxylase gene. J Biol Chem 269:10545–10550.

Ohyama Y, Ozono K, Uchida M, Yoshimura M, Shinki T, Suda T, Yamamoto O. 1996. Functional assessment of two vitamin D-responsive elements in the rat 25-hydroxyvitamin D_3 24-hydroxylase gene. J Biol Chem 271:30381–30385.

Oñate SA, Tsai SY, Tsai M-J, O'Malley BW. 1995. Sequence and characterization of a coactivator for the steroid hormone receptor superfamily. Science 270:1354–1357.

Pascussi JM, Gerbal-Chaloin S, Drocourt L, Maurel P, Vilarem MJ. 2003. The expression of CYP2B6, CYP2C9 and CYP3A4 genes: A tangle of networks of nuclear and steroid receptors. Biochim Biophys Acta 1619:243–253.

Pike JW. 1984. Monoclonal antibodies to chick intestinal receptors for 1,25-dihydroxyvitamin D_3. J Biol Chem 259:1167–1173.

Rachez C, Freedman LP. 2001. Mediator complexes and transcription. Curr Opin Cell Biol 13:274–280.

Rachez C, Suldan Z, Ward J, Chang CP, Burakov D, Erdjument-Bromage H, Tempst P, Freedman LP. 1998. A novel protein complex that interacts with the vitamin D_3 receptor in a ligand-dependent manner and enhances VDR transactivation in a cell-free system. Genes Dev 12:1787–1800.

Rachez C, Lemon BD, Suldan Z, Bromleigh V, Gamble M, Näär AM, Erdjument-Bromage H, Tempst P, Freedman LP. 1999. Ligand-dependent transcription activation by nuclear receptors requires the DRIP complex. Nature 398:824–828.

Rachez C, Gamble M, Chang CP, Atkins GB, Lazar MA, Freedman LP. 2000. The DRIP complex and SRC-1/p160 coactivators share similar nuclear receptor binding determinants but constitute functionally distinct complexes. Mol Cell Biol 20:2718–2726.

Rochel N, Wurtz JM, Mitschler A, Klaholz B, Moras D. 2000. The crystal structure of the nuclear receptor for vitamin D bound to its natural ligand. Mol Cell 5:173–179.

Rosenfeld MG, Glass CK. 2001. Coregulator codes of transcriptional regulation by nuclear receptors. J Biol Chem 276:36865–36868.

Scheidereit C, Geisse S, Westphal HM, Beato M. 1983. The glucocorticoid receptor binds to defined nucleotide sequences near the promoter of mouse mammary tumour virus. Nature 304:749–752.

Schmiedlin-Ren P, Thummel KE, Fisher JM, Paine MF, Lown KS, Watkins PB. 1997. Expression of enzymatically active CYP3A4 by Caco-2 cells grown on extracellular matrix-coated permeable supports in the presence of 1alpha,25-dihydroxyvitamin D_3. Mol Pharmacol 51: 741–754.

Schmiedlin-Ren P, Thummel KE, Fisher JM, Paine MF, Watkins PB. 2001. Induction of CYP3A4 by 1 alpha,25-dihydroxyvitamin D_3 is human cell line-specific and is unlikely to involve pregnane X receptor. Drug Metab Dispos 29:1446–1453.

Shulman AI, Larson C, Mangelsdorf DJ, Ranganathan R. 2004. Structural determinants of allosteric ligand activation in RXR heterodimers. Cell 116:417–429.

Spencer TE, Jenster G, Burcin MM, Allis CD, Zhou J, Mizzen CA, McKenna NJ, Onate SA, Tsai SY, Tsai MJ, O'Malley BW. 1997. Steroid receptor coactivator-1 is a histone acetyltransferase. Nature 389:194–198.

Staal A, van Wijnen AJ, Birkenhäger JC, Pols HAP, Prahl J, DeLuca H, Gaub M-P, Lian JB, Stein GS, van Leeuwen JPTM, Stein JL. 1996. Distinct conformations of vitamin D receptor/retinoid X receptor-α heterodimers are specified by dinucleotide differences in the vitamin D-responsive elements for the osteocalcin and osteopontin genes. Mol Endocrinol 10:1444–1456.

Staudinger JL, Goodwin B, Jones SA, Hawkins-Brown D, MacKenzie KI, LaTour A, Liu Y, Klaassen CD, Brown KK, Reinhard J, Willson TM, Koller BH, Kliewer SA. 2001. The nuclear receptor PXR is a lithocholic acid sensor that protects against liver toxicity. Proc Natl Acad Sci USA 98:3369–3374.

Sutton AL, MacDonald PN. 2003. Vitamin D: More than a 'bone-a-fide' hormone. Mol Endocrinol 17:777–791.

Terpening CM, Haussler CA, Jurutka PW, Galligan MA, Komm BS, Haussler MR. 1991. The vitamin D-responsive element in the rat bone gla protein is an imperfect direct repeat that cooperates with other *cis*-elements in 1,25-dihydroxyvitamin D_3-mediated transcriptional activation. Mol Endocrinol 5:373–385.

Thompson PD, Jurutka PW, Haussler CA, Whitfield GK, Haussler MR. 1998. Heterodimeric DNA binding by the vitamin D receptor and retinoid X receptors is enhanced by 1,25-dihydroxyvitamin D_3 and inhibited by 9-*cis* retinoic acid: Evidence for allosteric receptor interactions. J Biol Chem 273:8483–8491.

Thompson PD, Jurutka PW, Whitfield GK, Myskowski SM, Eichhorst KR, Encinas Dominguez C, Haussler CA, Haussler MR. 2002. Liganded VDR induces CYP3A4 in small intestinal and colon cancer cells via DR3 and ER6 vitamin D responsive elements. Biochem Biophys Res Commun 299:730–738.

Thummel KE, Brimer C, Yasuda K, Thottassery J, Senn T, Lin Y, Ishizuka H, Kharasch E, Schuetz J, Schuetz E. 2001. Transcriptional control of intestinal cytochrome P-450 3A by 1alpha,25-dihydroxy vitamin D_3. Mol Pharmacol 60:1399–1406.

Tocchini-Valentini G, Rochel N, Wurtz JM, Mitschler A, Moras D. 2001. Crystal structures of the vitamin D receptor complexed to superagonist 20-epi ligands. Proc Natl Acad Sci USA 98:5491–5496.

Tocchini-Valentini G, Rochel N, Wurtz JM, Moras D. 2004. Crystal structures of the vitamin D nuclear receptor liganded with the vitamin D side chain analogues calcipotriol and seocalcitol, receptor agonists of clinical importance. Insights into a structural basis for the switching of calcipotriol to a receptor antagonist by further side chain modification. J Med Chem 47:1956–1961.

Vanhooke JL, Benning MM, Bauer CB, Pike JW, DeLuca HF. 2004. Molecular structure of the rat vitamin D receptor ligand binding domain complexed with 2-carbon-substituted vitamin D_3 hormone analogues and a LXXLL-containing coactivator peptide. Biochemistry 43:4101–4110.

Watkins RE, Wisely GB, Moore LB, Collins JL, Lambert MH, Williams SP, Willson TM, Kliewer SA, Redinbo MR. 2001. The human nuclear xenobiotic receptor PXR: Structural determinants of directed promiscuity. Science 292:2329–2333.

Whitfield GK, Hsieh J-C, Nakajima S, MacDonald PN, Thompson PD, Jurutka PW, Haussler CA, Haussler MR. 1995. A highly conserved region in the hormone binding domain of the human vitamin D receptor contains residues vital for heterodimerization with retinoid X receptor and for transcriptional activation. Mol Endocrinol 9:1166–1179.

Whitfield GK, Selznick SH, Haussler CA, Hsieh J-C, Galligan MA, Jurutka PW, Thompson PD, Lee SM, Zerwekh JE, Haussler MR. 1996. Vitamin D receptors from patients with resistance to 1,25-dihydroxyvitamin D_3: Point mutations confer reduced transactivation in response to ligand and impaired interaction with the retinoid X receptor heterodimeric partner. Mol Endocrinol 10:1617–1631.

Whitfield GK, Jurutka PW, Haussler CA, Haussler MR. 1999. Steroid hormone receptors: Evolution, ligands and molecular basis of biologic function. J Cell Biochem Suppls 32(33):110–122.

Xie W, Radominska-Pandya A, Shi Y, Simon CM, Nelson MC, Ong ES, Waxman DJ, Evans RM. 2001. An essential role for nuclear receptors SXR/PXR in detoxification of cholestatic bile acids. Proc Natl Acad Sci USA 98:3375–3380.

Xu J, Li Q. 2003. Review of the in vivo functions of the p160 steroid receptor coactivator family. Mol Endocrinol 17:1681–1692.

Yoshizawa T, Handa Y, Uematsu Y, Takeda S, Sekine K, Yoshihara Y, Kawakami T, Arioka K, Sato H, Uchiyama Y, Masushige S, Fukamizu A, Matsumoto T, Kato S. 1997. Mice lacking the vitamin D receptor exhibit impaired bone formation, uterine hypoplasia and growth retardation after weaning. Nat Genet 16:391–396.

Zhang C, Dowd DR, Staal A, Gu C, Lian JB, van Wijnen AJ, Stein GS, MacDonald PN. 2003. Nuclear coactivator-62 kDa/Ski-interacting protein is a nuclear matrix-associated coactivator that may couple vitamin D receptor-mediated transcription and RNA splicing. J Biol Chem 278:35325–35336.

Zierold C, Darwish HM, DeLuca HF. 1994. Identification of a vitamin D-responsive element in the rat calcidiol (25-hydroxyvitamin D_3) 24-hydroxylase gene. Proc Natl Acad Sci USA 91:900–902.